

國立交通大學

電信工程研究所

碩士論文

多極化與多頻率可重置天線



Multiple Polarization and Multiple Frequency  
Reconfigurable Antenna

研究生：陳耿賢

指導教授：唐震寰 博士

中華民國九十九年七月

# 多極化與多頻率可重置天線

Multiple Polarization and Multiple Frequency Reconfigurable

Antenna

研究生：陳耿賢

Student : Keng-Hsien Chen

指導教授：唐震寰 博士

Advisor : Dr. Jenn-Hwan Tarnng

國立交通大學



A Thesis

Submitted to Institute of Communication Engineering

College of Electrical and Computer Engineering

National Chiao Tung University

in partial Fulfillment of the Requirements

for the Degree of Master of Science in

Communication Engineering

Hsinchu, Taiwan, Republic of China

中華民國九十九年七月

# 多極化與多頻率可重置天線

研究生：陳耿賢

指導教授：唐震寰 教授

國立交通大學

電信工程研究所 碩士班

## 摘要

可攜式行動通訊設備可應用可重置天線適當地調整天線的傳輸頻率或極化，抑制旁帶雜訊或改善極化不匹配的損失。可重置天線 (reconfigurable antennas) 設計之挑戰以最小的體積達到最多的頻率，極化或場型之選擇為目的。設計上，為降低成本，多採用PIN二極體的開關機制，產生多重電流路徑，達到天線的多頻率，極化或是場型的改變。不過如何在改變其中一個特性時，其他的特性能仍保持不變，例如，重置頻率時仍能保持原有的極化與輻射場型的特性，這將是一個挑戰。通常一個模態由一個PIN二極體所控制，所以，當要產生較多模態時，經常會使用多個PIN二極體，使得天線滿足上述需求。但是使用多個PIN二極體，將大幅的增加天線的成本，並且多個PIN二極體間的相互干擾/耦合，使得多模重置的設計變得相當困難。

本論文提出一個多頻率與極化重置天線。該天線僅使用四個PIN二極體開關的切換，即可達成五種可切換的模態，相較於其他可重置天線，具有體積小，低成本，與多重置的特性。該天線是由正方形的微帶天線和四片”耳型”的延伸金屬片所構成。每一個耳型金屬片與正方形微帶天線之間的連接，皆由一個PIN二極體的開關控制。透過適當地操控PIN二極體開關，改變電流路徑和改變橫向電磁波的模態，使天線產生不同的操作頻率或極化。取代以往由單一開關控制單一模式的型式，每一個開關可重複使用，使得僅用四個開關產生三個可切換的操作頻率，以及三個可切換的極化，適合用在小型的手持設備如智慧型手機或筆記型電腦等的相關產品。

# **Multiple Polarization and Multiple Frequency Reconfigurable Antenna**

Student : Keng-Hsien Chen

Advisor : Dr. Jenn-Hwan Tarng

Institute of Communication Engineering

National Chiao Tung University

## **Abstract**

**A novel multiple-ear patch antenna for polarization and frequency diversities is proposed. The proposed antenna uses the PIN diodes and adjacent ears, which are small adjacent patches, to achieve the diversities purposes. By connecting or disconnecting the ears and main patch, both of the resonant frequency and transverse magnetic (TM) of proposed antenna are changed to achieve the diversities. The proposed antenna has a compact size and simple structure, which comprises of a main patch antenna, four adjacent patches and four PIN diodes. With suitable arrangement of the bias network, the proposed antenna demonstrates either switching frequency in 3.2, 3.35 or 3.6GHz with the linear polarization (LP); or switching polarization in linear, right hand circular or left hand circular polarization (RHCP/ LHCP) in the same frequency. The simulated and measured results reveal good impedance bandwidth, axial ratio, and radiation patterns; hence the proposed reconfigurable mechanism is well suited for wireless communication applications.**

## 誌 謝

在碩士班研究的這二年歲月，首先要感謝的是我的指導教授 唐震寰教授並致上我最誠摯的謝意。感謝老師在專業領域中，給予我不斷的指導與鼓勵，並賦予了實驗室豐富的研究資源與環境，使得這篇碩士論文能夠順利完成。同時，亦感謝口試委員元智大學 彭松村教授、國立台灣科技大學 楊成發教授及國立台北科技大學 林丁丙教授對於論文內容所提出的寶貴建議及指導，在此致上最誠懇的謝意。

其次，要感謝實驗室的學長們——松融學長、瑞榮學長、文崇學長、雅仲學長、俊諺學長、菘菲學長、宗霖學長、兆凱學長、振銘學長、明宗學長、廣琪學長等在研究上的幫助與意見，讓我獲益良多。感謝實驗室的同學——鈺宏、冠豪、國政等在課業及研究上的互相砥礪與切磋，以及生活上的多彩多姿，另外要感謝炳志、育正、庭榜、健候、曉晴、漢維等在量測天線時的幫忙。亦感謝學弟們——昌喆、佳迪、詠舜、啟宏，讓實驗室在嚴肅的研究氣氛中增添了許多歡樂，有了你們，更加豐富了我這二年的研究生生活。另外，也要感謝助理——梁麗君小姐，在實驗室上的協助和籌劃每次的美食聚餐饗宴。

最後，要感謝的就是我最親愛的家人。他們在我求學過程中，一路陪伴著我，給予我最溫馨的關懷與鼓勵，讓我在人生的過程裡得到快樂，更讓我可以專心於研究工作中而毫無後顧之憂。

鑒此，謹以此篇論文獻給所有關心我的每一個人。

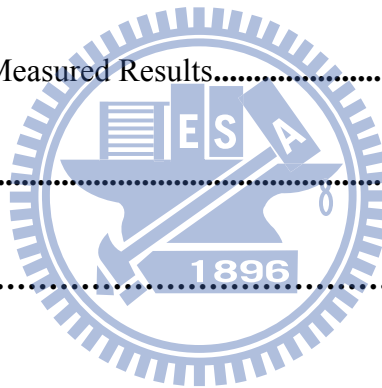
陳耿賢 誌予

九十九年七月

# Contents

<b>Abstract (Chinese)</b> .....	<b>I</b>
<b>Abstract (English)</b> .....	<b>II</b>
<b>Acknowledgement</b> .....	<b>III</b>
<b>Contents</b> .....	<b>IV</b>
<b>List of figures</b> .....	<b>VI</b>
<b>List of tables</b> .....	<b>VIII</b>
<b>Chapter 1 Introduction</b> .....	<b>1</b>
1.1 Background.....	1
1.2 Related Works.....	2
1.3 Organization of Thesis.....	3
<b>Chapter 2 Introduction of Microstrip patch Antennas</b> .....	<b>5</b>
2.1 Introduction .....	5
2.2 Antenna Parameters .....	5
2.3 Microstrip Antenna.....	6
<b>Chapter 3 Multiple-Ear Patch Antenna for Polarization and Frequency Diversities ....</b>	<b>10</b>
3.1 Introduction .....	10
3.2 Antenna Configuration and Design Concept.....	13
3.2.1 Antenna Configuration and Operating Mechanism.....	13
3.2.2 Frequency Reconfigurability .....	16
3.2.3 Polarization Reconfigurability.....	18

3.3	PARAMETRIC STUDY AND RADIATION CHARACTERISTICS .....	22
3.3.1	Parametric Study .....	22
3.3.2	Radiation Characteristics .....	25
<b>Chapter 4</b>	<b>Conclusion .....</b>	<b>27</b>
<b>Appendix A</b>	<b>Introduction of Slot Antennas.....</b>	<b>28</b>
<b>Appendix B</b>	<b>Frequency Reconfigurable Slot Antenna Using PIN Diodes.....</b>	<b>35</b>
B.1	Introduction .....	35
B.2	Antenna Configuration and Design Concept.....	36
B.3	Simulated and Measured Results.....	37
B.4	Conclusion.....	40
<b>References</b>	.....	<b>43</b>



## List of Figures

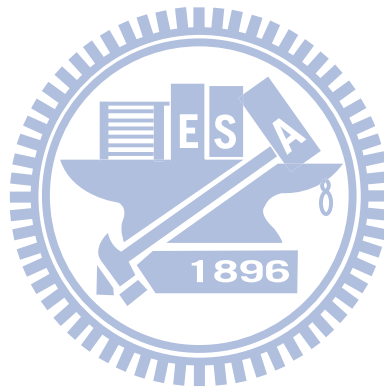
<p><b>Fig. 2-1. (a) Geometry for analyzing the edge-fed microstrip patch antenna. (b) Side view showing the electric fields. (c) Top view showing the fringing electric fields that are responsible for radiation. The equivalent magnetic surface <math>M_s</math> currents are also shown.....</b></p>	<p><b>9</b></p>
<p><b>Fig. 3-1. Geometry of the proposed antenna. (a) Top view. (b) Cross-sectional view.....</b></p>	<p><b>12</b></p>
<p><b>Fig. 3-2. The operating mechanism of the proposed antenna for (a) <math>FR_h</math>, (b) <math>FR_l</math>, (c) <math>FR_{mid}</math> or <math>PR_{lp}</math>, (d) <math>PR_{lhcp}</math>, or (e) <math>PR_{rhcp}</math>.....</b></p>	<p><b>13</b></p>
<p><b>Fig. 3-3. Conceptual schematic of the dc bias networks .....</b></p>	<p><b>15</b></p>
<p><b>Fig. 3-4. Simulated and measured <math>S_{11}</math> for FR scheme. ....</b></p>	<p><b>16</b></p>
<p><b>Fig. 3-5. Simulated and measured <math>S_{11}</math> for PR scheme. ....</b></p>	<p><b>17</b></p>
<p><b>Fig. 3-6. Simulated and measured axial ratio for PR scheme.....</b></p>	<p><b>18</b></p>
<p><b>Fig. 3-7. (a) Simulated <math>S_{11}</math> for different <math>W_1</math> in <math>FR_l</math>. (b) Simulated <math>S_{11}</math> for different <math>L_5</math> in <math>FR_l</math>. ....</b></p>	<p><b>19</b></p>
<p><b>Fig. 3-8. (a) Simulated <math>S_{11}</math> for different <math>L_5</math> in <math>PR_{lhcp}</math>. (b) Simulated axial ratio for different <math>L_5</math> in <math>PR_{lhcp}</math>.....</b></p>	<p><b>20</b></p>
<p><b>Fig. 3-9. (a) Simulated <math>S_{11}</math> for different <math>L_4</math> in <math>PR_{lhcp}</math>. (b) Simulated axial ratio for different <math>L_4</math> in <math>PR_{lhcp}</math>.....</b></p>	<p><b>20</b></p>
<p><b>Fig. 3-10. Simulated surface current distribution of (a) <math>FR_l</math>, (b) <math>FR_{mid}</math>, (c) <math>FR_h</math>, (d) <math>PR_{rhcp}</math>, and (e) <math>PR_{lhcp}</math>. ....</b></p>	<p><b>21</b></p>



<b>Fig. 3-11. Photograph of (a) the front side and (b) the back side of fabricated antenna.</b>	<b>23</b>
<b>Fig. 3-12. Simulated and measured radiation patterns for (a) <math>PR_{mid}</math>, (b) <math>PR_{lhcp}</math>, and (c) <math>PR_{rhcp}</math> (unit : dBi) .....</b>	<b>24</b>
<b>Fig. 3-13. The simulated and measured axial ratio at 3.35GHz for <math>PR_{lhcp}</math> and <math>PR_{rhcp}</math>.....</b>	<b>25</b>
<b>Fig. A-1. The stubs of (a) are a poor radiator, the slot of (b) is a good, efficient radiator. (c) and (d) are slot antennas fed by coaxial transmission lines.....</b>	<b>29</b>
<b>Fig. A-2. A layout of microstrip-to-slot transition.....</b>	<b>30</b>
<b>Fig. A-3. Transmission line equivalent circuit for the transition of Fig. A-2.....</b>	<b>30</b>
<b>Fig. A-4. Reduced equivalent circuit of Fig. A-3.....</b>	<b>30</b>
<b>Fig. A-5. Transformed equivalent circuit of Fig. A-4.....</b>	<b>31</b>
<b>Fig. A-6. Geometry of a microstrip-fed quarter-wavelength slot antenna. ....</b>	<b>34</b>
<b>Fig. B-1. (a) Configuration of proposed antenna. (b) PIN diodes arrangement and the associated dc bias network.....</b>	<b>36</b>
<b>Fig. B-2. Return loss of proposed antenna. (a) LR mode. (b) RR mode.....</b>	<b>38</b>
<b>Fig. B-3. Simulated current distribution. (a) LR mode. (b) RR mode.....</b>	<b>39</b>
<b>Fig. B-4. Return loss of proposed antenna at <math>W1=W4=13.75mm</math>.....</b>	<b>39</b>
<b>Fig. B-5. Simulated and measured radiation patterns. (a) xy-plane. (b) xz-plane. (c) yz-plane.....</b>	<b>42</b>

## List of Tables

Table 3-I Frequency reconfigurable scheme .....	14
Table 3-II Polarization reconfigurable scheme .....	14



## Chapter 1 *Introduction*

---

### 1.1 Background

With advances in technology, wireless communication has become an integral part of daily life. For example, wireless local area networks (WLAN), wireless personal area networks (WPAN), and RFID systems, all sorts of wireless applications makes people's lives more convenient than the past. Antennas play an important role in wireless communications. The performance of the antenna will affect the communication quality.

With the increase of wireless applications and rapid development of technology, wireless communications desire antennas with frequency diversity and polarization diversity to adapt in different application platforms and to improve polarization mismatch loss. Antennas with frequency diversity, such as multi-band or broadband antennas, make antennas operate in different frequency bands to transmit and receive messages in various telecommunication services. Polarization diversity can improve the communication quality when receiving signal, so the signal will not suffer from multipath diffraction or scattering, resulting in polarization mismatch loss, such as using different polarization antenna to achieve polarization diversity. Pattern diversity, controlling null position in the radiation patterns, can avoid receiving noise from other devices and transmitting signals to unrelated devices, such as using antenna arrays

to achieve pattern diversity.

Although multiband or broadband antennas can operate in different frequencies, they receive unwanted signals from other frequency bands, which makes the system require stringent filters and results in increasing costs and space requirement. Different polarization antennas can receive signals with various polarizations which minimize the polarization mismatch loss. However, using multiple antennas will greatly increase the space requirement. Array antennas, which consist of a number of antennas, due to space constraints and multiple antenna coupling effect, are not suitable for application in handheld devices.

## **1.2 Related Works**

In recent years, software defined radio (SDR) and cognitive radio (CR) have received significant attention in the field of wireless communications. The SDR/CR device changes its transmission or reception parameters to communicate efficiently between licensed and unlicensed users. These parameters include operating frequency, spectrum, signal format modulation, etc. Hence, some researchers proposed reconfigurable antennas to be a good front-end solution to accompany the development of SDR/CR networks [1]. These reconfigurable antennas are capable of achieving diversity in the operating frequencies, polarizations, radiation patterns as well as gain; therefore, these antennas can fulfill the requirements of SDR/CR networks. Moreover, signals in the real world suffer multipath, fading, and diffraction as well as interference. The wireless system uses the reconfigurable antenna to increase the signal-to-noise ratio of the whole system by achieving diversity capabilities.

Generally, reconfigurable antennas are categorized in terms of frequency, radiation pattern, or polarization. The frequency reconfigurable antenna changes operating frequency

while maintaining radiation characteristics. Compared to multiband antennas, the frequency reconfigurable antenna could be used in the multiband communication system for better out-of-band rejection. The frequency reconfigurable antenna only has one operating frequency in each operation. In other words, it has inherent bandpass characteristics that eliminates the demand of an isolated filter and hence reduces the front-end circuit complexity [2]-[5]. Consequently, the pattern reconfigurable antenna which changes radiation pattern while maintaining operating frequency and bandwidth can greatly enhance system performance by steering its radiation beams or nulls in several predefined reception directions. Therefore, it also achieves angle/space diversity at a given operating frequency. Pattern reconfigurable antennas are applied in handheld devices to decrease the interference with other devices and to improve communication quality [6]-[8]. A pattern reconfigurable bow-tie antenna using a CPW-to-slot line transition and a switchable polarization patch antenna have been investigated to increase the signal-to-noise (SNR) ratio [9]-[11]. Finally, the polarization reconfigurable antenna has been reported in [12]-[21]. Such antennas are commonly designed based on the microstrip patch antenna with truncated corners or slots so as to switch the antenna polarization states between RHCP, LHCP, LP, vertical polarization, or horizontal polarization.

### **1.3 Organization of Thesis**

The thesis is organized as follows.

Chapter 2: The essential backgrounds are described. It starts from antenna parameters in antenna design. And then the introduction of microstrip antennas is given.

Chapter 3: A novel multiple-ear patch antenna for polarization and frequency diversities is

proposed. The antenna configuration, design concept, and bias network are described firstly. The parameter study and the antenna operating mechanism is also described and explored. Next, the simulated and measured results such as axial ratio and radiation patterns are presented.

#### Chapter 4: Conclusion

The previous work (a frequency reconfigurable slot antenna using PIN diodes) of multiple-ear patch antenna for polarization and frequency diversities is given in appendixes.

Appendix A: Introduction of slot antenna.

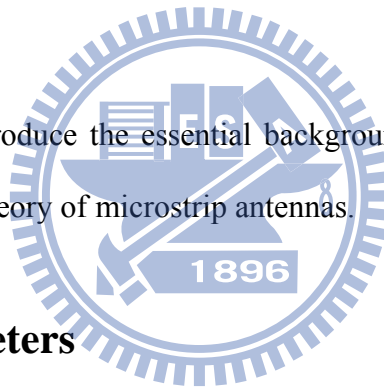
Appendix B: A frequency reconfigurable slot antenna using PIN diodes is proposed. The proposed antenna structure and design concept are presented firstly. And then the measured and simulated results of the proposed antenna such as return loss and radiation patterns are given. Finally, it is a brief summary.

## Chapter 2 *Introduction of Microstrip patch Antennas*

---

### 2.1 Introduction

In this chapter, we introduce the essential background for the antenna design, such as antennas parameters and theory of microstrip antennas.



### 2.2 Antenna Parameters

- Directivity  $D$  — a ratio of the maximum power density in the main beam direction to the average radiated power density.
- Radiation Efficiency  $\eta$  — a ratio of radiated power to the input power.
- Gain  $G$  — a ratio of the maximum radiation intensity to the radiation intensity obtained if power received by the antenna were radiated isotropically.
- VSWR — Voltage Standing Wave Ratio, is a measure of how efficiently radio-frequency power is transmitted from a power source, through a transmission

line, into a load.

- Return Loss or Reflection Coefficient  $\Gamma$  — a loss of signal power results from the reflection caused at a discontinuity in a transmission line or optical fiber. Return loss is usually expressed in dB and equals to  $-20\log(\Gamma)$ . Reflection Coefficient is a ratio of the amplitude of the reflected wave to the amplitude of the incident wave.
- Bandwidth — a range of frequencies over which important performance parameters are acceptable. (frequencies were determined by the  $VSWR \leq 2$ )
- Polarization — the orientation of oscillations in the plane perpendicular to a transversal wave's direction of travel. Antenna polarizations: Linear, Circular, Elliptical.
- Radiation Pattern — angular variation of radiation around the antenna, including: Directive, single or multiple narrow beams, Omnidirectional (uniform radiation in one plane), Shaped main beam

## 2.3 Microstrip Antenna

Microstrip antennas have several advantages compared to conventional micro-wave antennas, such as light weight, low volume, thin profile configurations, low fabrication cost, and readily amenable to mass production. Based on these advantages, microstrip patch antenna become one of the most common form of printed antennas and were conceived in the 1950s. Extensive investigation of patch antennas began in the 1970s [22],[23] and resulted in many useful design configurations [24].



Fig. 2-1 shows the most commonly used microstrip antenna, a rectangular patch being fed from a microstrip transmission line. The fringing fields act to extend the effective length of the patch. Thus, the length of a half-wave patch is slightly less than a half wavelength in the dielectric substrate material. An approximate value for the length of a resonant half-wavelength patch is [23].

$$L \approx 0.49\lambda_d = 0.49 \frac{\lambda}{\sqrt{\epsilon_r}} \quad \text{Half-Wavelength patch}$$

The region between the conductors acts as a half-wavelength transmission line cavity that is open-circuited at its ends and the electric fields associated with the standing wave mode in the dielectric. In Fig. 2-1(b), the fringing field at the ends are exposed to the upper half-space ( $Z>0$ ) and are responsible for the radiation. The standing wave mode with a half-wavelength separation between ends leads to electric fields that are of opposite phase on the left and right halves. The x-components of the fringing fields are actually in-phase, leading to a broadside radiation pattern. This model suggests an “aperture field” analysis approach where the patch has two radiation slot aperture with electric fields in the plane of the patch. For the half-wavelength patch case, the slots are equal in magnitude and phase. The patch radiation is linearly polarization in the xz-plane, that is, parallel to the electric fields in the slots. Pattern computation for the rectangular patch is easily performed by first creating equivalent magnetic surface currents as shown in Fig. 2-1(c). If we assume the thickness of the dielectric material  $t$  is small, the far-field components follow from the equations as

$$E_\theta = E_o \cos \phi f(\theta, \phi)$$

$$E_\phi = -E_o \cos \theta \sin \phi f(\theta, \phi)$$

Where

$$f(\theta, \phi) = \frac{\sin\left[\frac{\beta W}{2} \sin\theta \sin\phi\right]}{\frac{\beta W}{2} \sin\theta \sin\phi} \cos\left(\frac{\beta L}{2} \sin\theta \cos\phi\right)$$

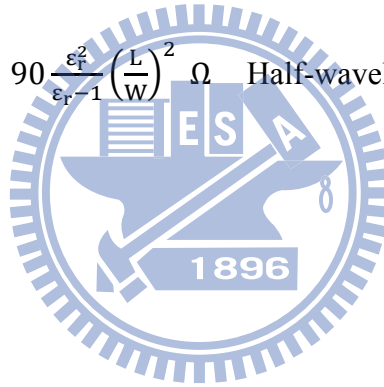
And  $\beta$  is the usual free-space phase constant. The principal plane pattern follows from as

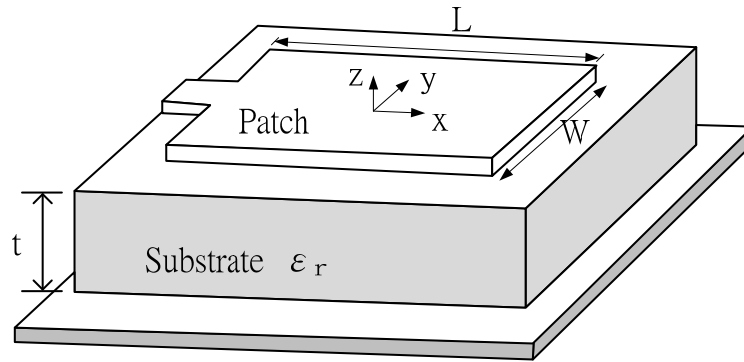
$$F_E(\theta) = \cos\left(\frac{\beta L}{2} \sin\theta\right) \quad \text{E-plane, } \phi = 0^\circ$$

$$F_H(\theta) = \cos\theta \frac{\sin\left[\frac{\beta W}{2} \sin\theta\right]}{\frac{\beta W}{2} \sin\theta} \quad \text{H-plane, } \phi = 90^\circ$$

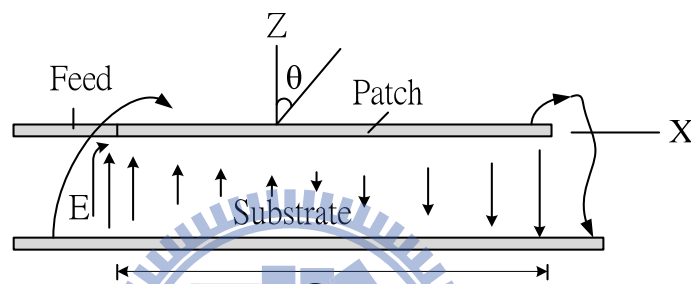
The patch width  $W$  is selected to give the proper radiation resistance at the input, often 50 ohms. An approximate expression for the input impedance of a resonant edge-fed patch is

$$Z_A = 90 \frac{\epsilon_r^2}{\epsilon_r - 1} \left(\frac{L}{W}\right)^2 \Omega \quad \text{Half-wavelength patch}$$

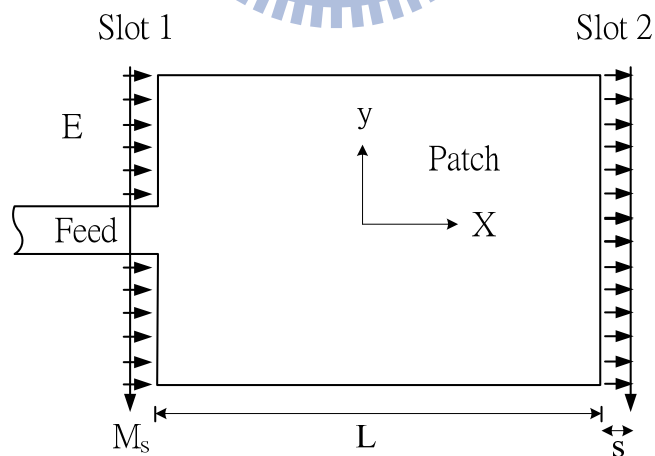




(a)



(b)



(c)

Fig. 2-1. (a) Geometry for analyzing the edge-fed microstrip patch antenna. (b) Side view showing the electric fields. (c) Top view showing the fringing electric fields that are responsible for radiation. The equivalent magnetic surface  $M_s$  currents are also shown.

## Chapter 3 *Multiple-Ear Patch Antenna for Polarization and Frequency Diversities*

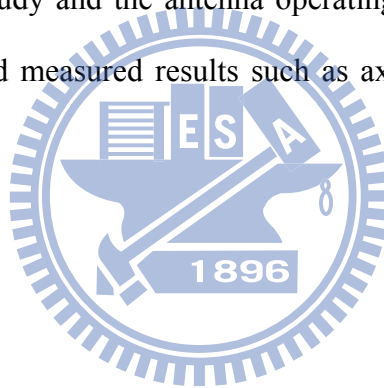
---

### 3.1 Introduction

Although reconfigurable antennas are well investigated in the antenna community, antennas simultaneously processing two of the aforementioned three reconfigurabilities (in Chapter 1) are sometimes quite limited owing to complex interaction of antenna structure, antenna mechanism or radiation characteristics. Hence, relatively few works have proposed. In [25], the patch antenna with switchable slot (PASS) is capable of selecting the two frequencies with RHCP, or LHCP, but it has to change the feed position to achieve polarization switching. In [26], a reconfigurable microstrip patch antenna with frequency and polarization diversities was proposed, but it has an extra quarter-wavelength impedance matching network which increases the antenna size. In [27], the single-feed circular microstrip antenna is able to control all three polarization modes (LHCP/RHCP/LP) at the same frequency, and one additional frequency with LP. However, this antenna consists of five switches (PIN diodes), and three matching stubs, which increase the cost and the size of the antenna at the same time. The problems of combining two distinct diversities together result from different characteristic of each diversity, and the difficulties of controlling diversity

functions in a limited space. Furthermore, because strong interaction between two diversity functions is blocked, one antenna with more than two diversity functions becomes hard to achieve.

In this chapter, a polarization and frequency reconfigurable patch antenna is proposed. The proposed antenna structure comprises of a main patch antenna, four adjacent patches, and four PIN diodes. Each PIN diode is located between the main patch antenna and an adjacent patch. By applying forward bias or reverse bias to the four PIN diodes, the proposed antenna demonstrates the frequency and polarization reconfigurable ability without an extra feed line or matching networks. In 3.2, the antenna configuration, design concept, and bias network are discussed. The parameter study and the antenna operating mechanism is also described and explored. The simulated and measured results such as axial ratio and radiation patterns are presented in 3.3.



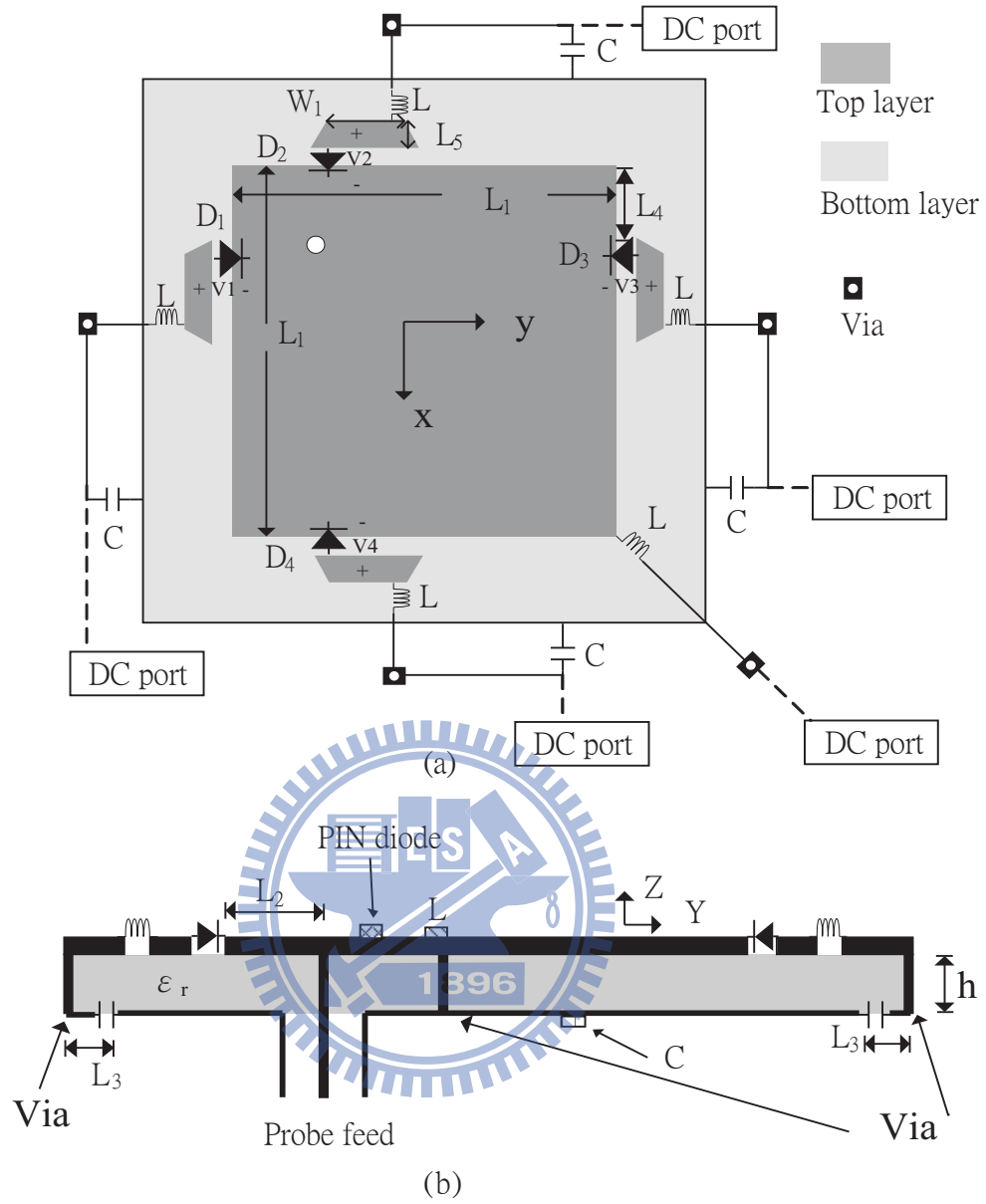


Fig. 3-1. Geometry of the proposed antenna. (a) Top view. (b) Cross-sectional view.

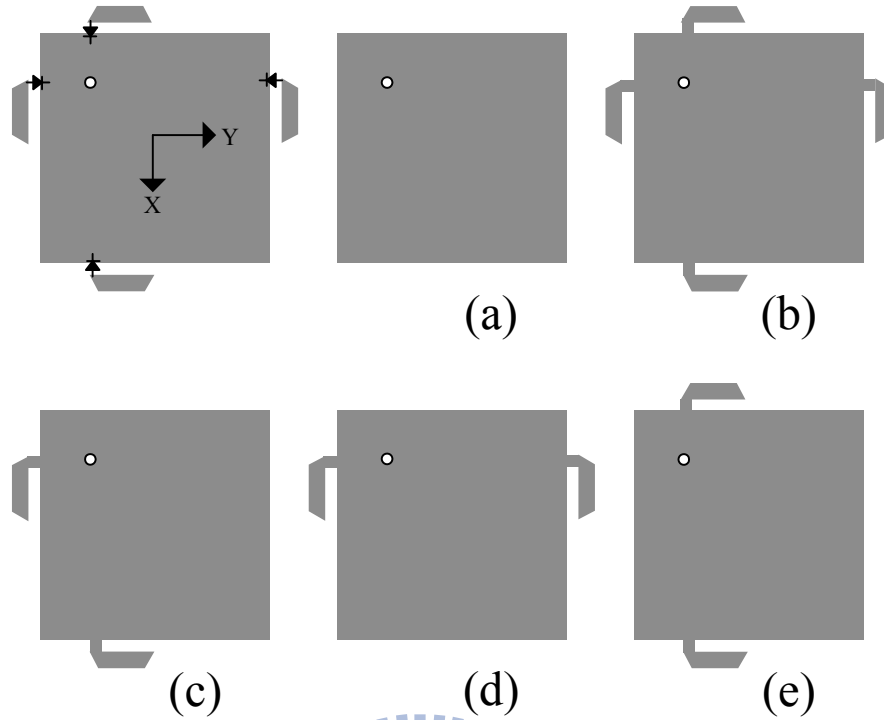


Fig. 3-2. The operating mechanism of the proposed antenna for (a)  $FR_h$ , (b)  $FR_l$ , (c)  $FR_{mid}$  or  $PR_{lp}$ , (d)  $PR_{lhcp}$ , or (e)  $PR_{rhcp}$ .

## 3.2 Antenna Configuration and Design Concept

### 3.2.1 Antenna Configuration and Operating Mechanism

The structure and operation mechanism of the proposed antenna for frequency and polarization reconfigurable purposes are shown in Fig. 3-1 and Fig. 3-2. The signal is fed directly to the diagonal line of the main patch antenna via an SMA connector. The PIN diodes are across the 0.5mm gap between main patch antenna and each adjacent patch. The patches are located on the opposite side of the main patch antenna. They are positioned near the main patch antenna and can provide either extended current path for frequency reconfigurable ability or changed transverse magnetic (TM) mode of the main patch antenna for polarization reconfigurable ability. The proposed antenna is etched on  $30 \times 30 \text{ mm}^2$  (total size) printed

circuit board (PCB) with  $h=1.6\text{mm}$  and  $\epsilon_r = 4.4$ . In this design, the PIN diode is BAR64-02V with a forward bias resistance of  $2.1 \Omega$  and reverse bias total capacitance of less than  $0.18\text{pF}$ . The DC bias voltage  $V_{DD}$  is either  $3\text{V}$  or  $-3\text{V}$  and is controlled by a finger switch for convenient operation. The power source is selected as coin cell batteries for measurement purpose. The current-limited resistors,  $R_1$  to  $R_4$ , are  $470 \text{ ohm}$  and hence the diode current  $I_D$  is from  $0.1\text{nA}$  to  $10 \text{ mA}$  which is dependent on the diode states. The final antenna parameters are as follows:  $L_1=19$ ,  $L_2=6$ ,  $L_3=4.5$ ,  $L_4=3.75$ ,  $L_5=2$ ,  $h=1.6$ ,  $W_1=4$ . (Unit: mm)

Table 3-I Frequency reconfigurable scheme

Freq. scheme	$D_1 / V_1$	$D_2 / V_2$	$D_3 / V_3$	$D_4 / V_4$	Freq.	Pol.
					(GHz)	
$FR_h$	OFF (-3V)	OFF (-3V)	OFF (-3V)	OFF (-3V)	3.6	LP
$FR_{mid}$	ON (3V)	OFF (-3V)	OFF (-3V)	ON (3V)	3.35	LP
$FR_l$	ON (3V)	ON (3V)	ON (3V)	ON (3V)	3.2	LP

Table 3-II Polarization reconfigurable scheme

Pol. scheme	$D_1$	$D_2$	$D_3$	$D_4$	Freq.	Pol.
	$/V_1$	$/V_2$	$/V_3$	$/V_4$	(GHz)	
$PR_{lhcp}$	OFF (-3V)	ON (3V)	OFF (-3V)	ON (3V)	3.35	LHCP
$PR_{rhcp}$	ON (3V)	OFF (-3V)	ON (3V)	OFF (-3V)	3.35	RHCP
$PR_{lp}$	ON (3V)	OFF (-3V)	OFF (-3V)	ON (3V)	3.35	LP



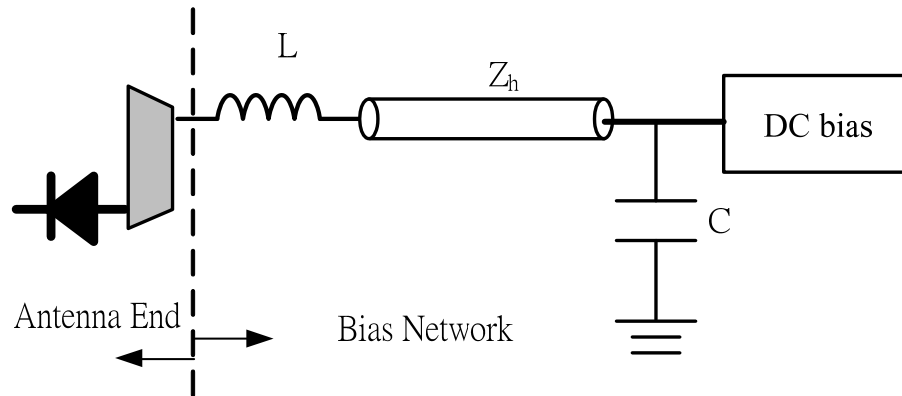


Fig. 3-3. Conceptual schematic of the dc bias networks

Table 3-I and Table 3-II illustrate the DC bias configuration for the frequency and polarization reconfigurable schemes. When the antenna is intended to be operated in frequency reconfigurable (FR) scheme—namely high, middle, and low, all the diodes are turned off for higher operating frequency ( $FR_h$ ) and all turned on for lower operating frequency ( $FR_l$ ), respectively. In addition, either  $D_1$  or  $D_4$  are turned on while  $D_2$  and  $D_3$  are turned off or  $D_1$  and  $D_4$  are turned off while  $D_2$  and  $D_3$  are turned on for middle operating frequency ( $FR_{mid}$ ). In the frequency reconfigurable schemes, the adjacent patches and PIN diodes are used to change the current distribution on the proposed antenna. Consequently, when the antenna is operated in a polarization reconfigurable (PR) scheme—namely, linear polarization ( $PR_{lp}$ ), right hand circular polarization ( $PR_{rhcp}$ ) or left hand circular polarization ( $PR_{lhcp}$ )— $D_1$  and  $D_3$  are turned on while  $D_2$  and  $D_4$  are turned off for left hand circular polarization or  $D_1$  and  $D_3$  are turned off while  $D_2$  and  $D_4$  are turned on for right hand circular polarization. In Table 3-II, the status of  $PR_{lp}$  is completely the same as  $FR_{mid}$  but they are named differently for easy understanding and comparison. The adjacent patches and PIN diodes affect the phase relationship between  $TM_{01}$  and  $TM_{10}$  in the PR purpose. In this work, the proposed antenna is intentionally designed to sufficiently achieve the above-mentioned abilities in the small frequency because the adjacent patches are too small and the

performance of proposed antenna is easily interfered with by the DC power line/source. The equivalent circuit diagram is shown in Fig. 3-3. As shown in Fig. 3-3, the path is comprised of diodes, adjacent patches, 18nH inductors, DC lines (high impedance lines), and 100pF capacitors. The 100pF capacitor is placed approximately one-quarter wavelength from the adjacent patch in order to block RF signals at adjacent patches and hence improve the RF-dc signal isolation. The value of inductor and capacitor is selected by the simulated result. In the simulation, a diode in the forward state is modeled as a 0.6nH inductor in series with a 2.1  $\Omega$  resistor, whereas a diode in reverse bias is modeled as 0.6nH inductor in series with a 3k $\Omega$  resistor and a 0.18pF capacitor in parallel. The above configuration ensures that the DC line/network cannot affect the antenna performance.

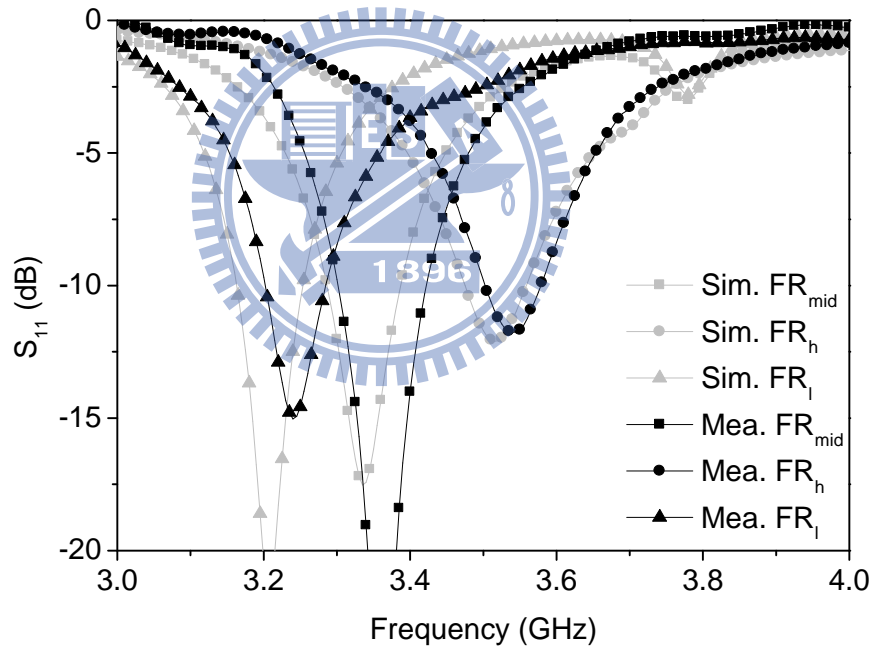


Fig. 3-4. Simulated and measured  $S_{11}$  for FR scheme.

### 3.2.2 Frequency Reconfigurability

The  $S_{11}$  of the proposed antenna for frequency reconfigurable purpose is shown in Fig. 3-4. The simulated and measured results are fair agreement and were taken by the Ansoft HFSS and the E8364B PNA network analyzer, respectively. In experiment, and  $FR_l$  is

determined by current flows to adjacent patches when the diodes are turned on, resulting in a longer resonant length. The operating frequency is determined by Eq. 3-1 to 3-3.

$$f \approx \frac{c}{\sqrt{\epsilon_{eff}} \cdot 2L} \quad (3-1)$$

$$\epsilon_{eff} = \frac{\epsilon_r + 1}{2} \quad (3-2)$$

$$L \approx L_{main} + L_{adjacent} \quad (3-3)$$

$L_{main}$  is the edge length of main patch antenna and approximates half wavelength of fundamental frequency. The  $L_{adjacent}$  is the length of extended current flow through the adjacent patch and is the dominated element for shifting operating frequency. The increment of operating frequency is simply in reverse proportion to  $L_{adjacent}$ . It is noted that the diode slightly shift the operating frequency to lower because it can be treated as an inductor and a resistor in series.

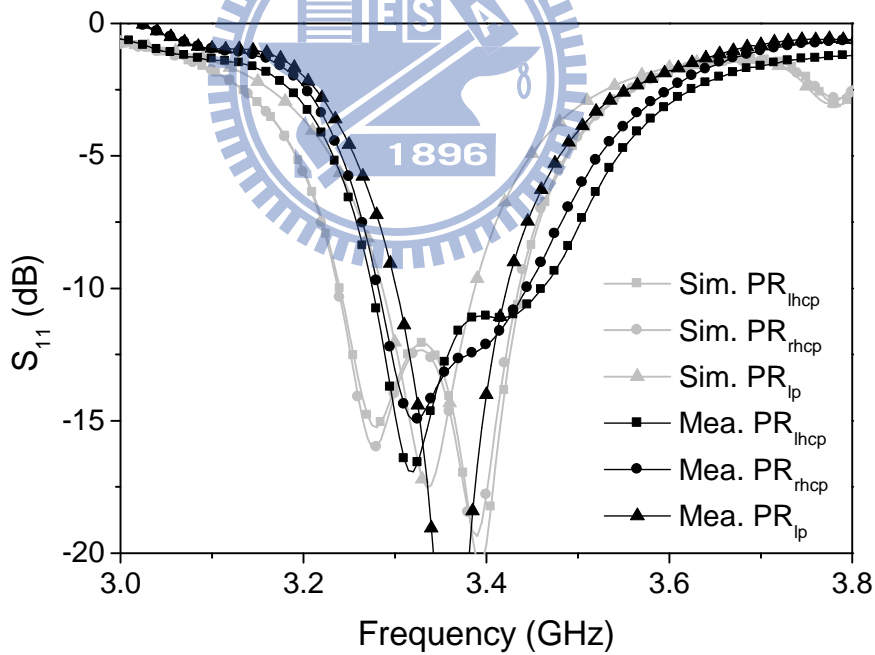


Fig. 3-5. Simulated and measured  $S_{11}$  for PR scheme.

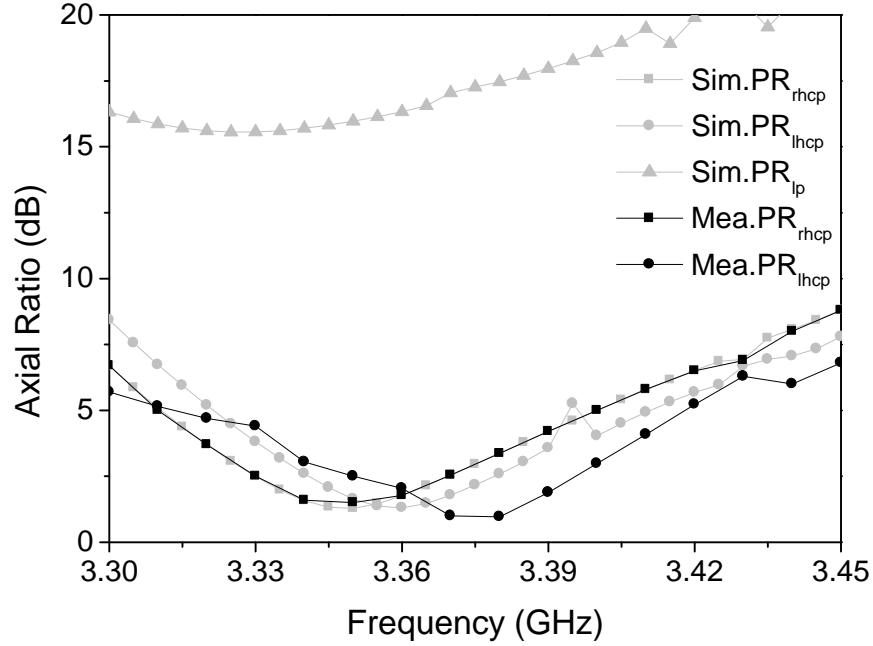


Fig. 3-6. Simulated and measured axial ratio for PR scheme.

### 3.2.3 Polarization Reconfigurability

The  $S_{11}$  and AR (Axial Ratio) of proposed antenna for polarization reconfigurable purpose are shown in Fig. 3-5 and Fig. 3-6, respectively. The measured results agree with the simulated ones. For  $PR_{rhcp}$  and  $PR_{lhcp}$ , the accepted operating bandwidths are 160 MHz and 195 MHz; meanwhile, the associated  $AR < 3$  bandwidths are 45 MHz and 55 MHz. The patch antenna can be described as a cavity with  $TM_{01}$  and  $TM_{10}$  modes [27], [28], on the other hand, the SMA feed is directly located on the diagonal line to excite two orthogonal modes. When  $TM_{10}$  and  $TM_{01}$  with equal amplitudes and 90 degrees phase difference are well designed, the LHCP or RHCP can be generated.

The most important parameters which affect the polarization are SMA feed location and the shapes of the main patch antenna and the adjacent patches. In the case of LHCP, the electric current flows along y-direction through the  $D_1$  and  $D_3$  and two adjacent patches, resulting longer resonant length than current flows along x-direction in the main patch only. This indicates that the y-polarized field leads the x-polarized field. By adjusting the length of

adjacent patches, the amplitude and phase relationship between  $TM_{01}$  and  $TM_{10}$  are obtained by

$$Amp_{01} = Amp_{10}$$

$$\phi_{01} - \phi_{10} = 90^\circ$$

In contrast, the case of RHCP, i.e., the x-polarized field leads the y-polarized field. When the antenna topology is properly designed, the  $TM_{10}$  and  $TM_{01}$  have the same amplitude and phase relationship given by

$$\phi_{01} - \phi_{10} = -90^\circ$$

Therefore, the RHCP is generated. Finally when phase relationship does not remain  $\pm 90^\circ$ , the polarization of the proposed antenna is linear polarization (LP). It is noted that the polarization reconfigurability can also implement by changing the width and length of the main patch antenna without the adjacent patches. On the other hand, the proposed antenna utilizes adjacent patches to obtained more flexibility in the reconfigurable antenna design for the different purposes.

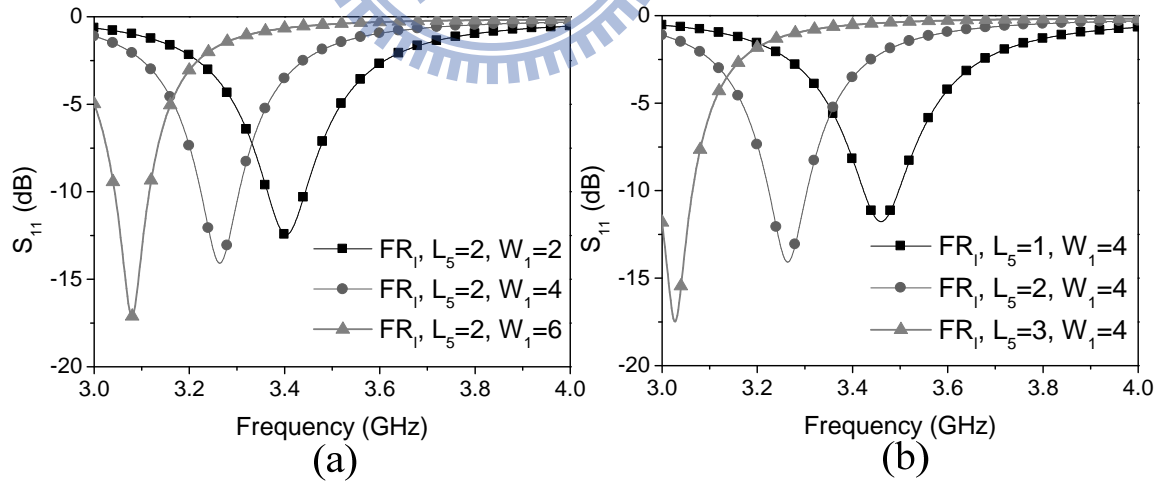


Fig. 3-7. (a) Simulated  $S_{11}$  for different  $W_1$  in  $FR_1$ . (b) Simulated  $S_{11}$  for different  $L_5$  in  $FR_1$ .

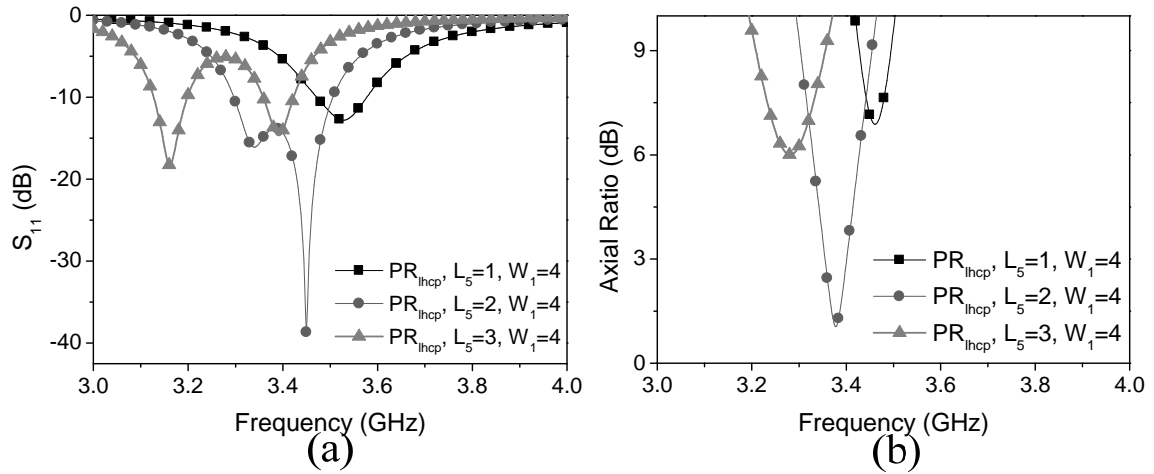


Fig. 3-8. (a) Simulated  $S_{11}$  for different  $L_5$  in  $PR_{lhcp}$ . (b) Simulated axial ratio for different  $L_5$  in  $PR_{lhcp}$ .

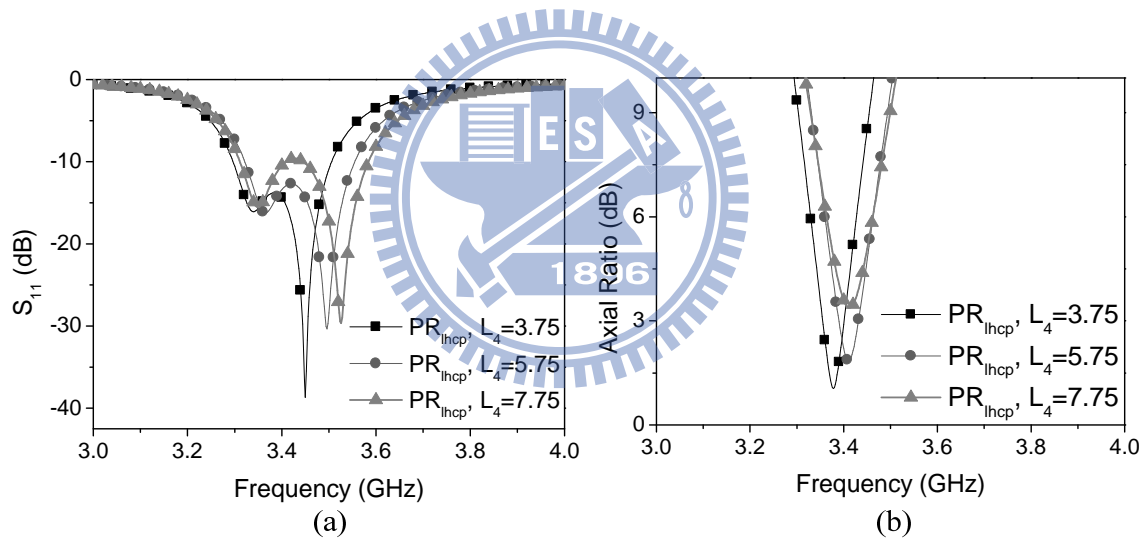


Fig. 3-9. (a) Simulated  $S_{11}$  for different  $L_4$  in  $PR_{lhcp}$ . (b) Simulated axial ratio for different  $L_4$  in  $PR_{lhcp}$ .

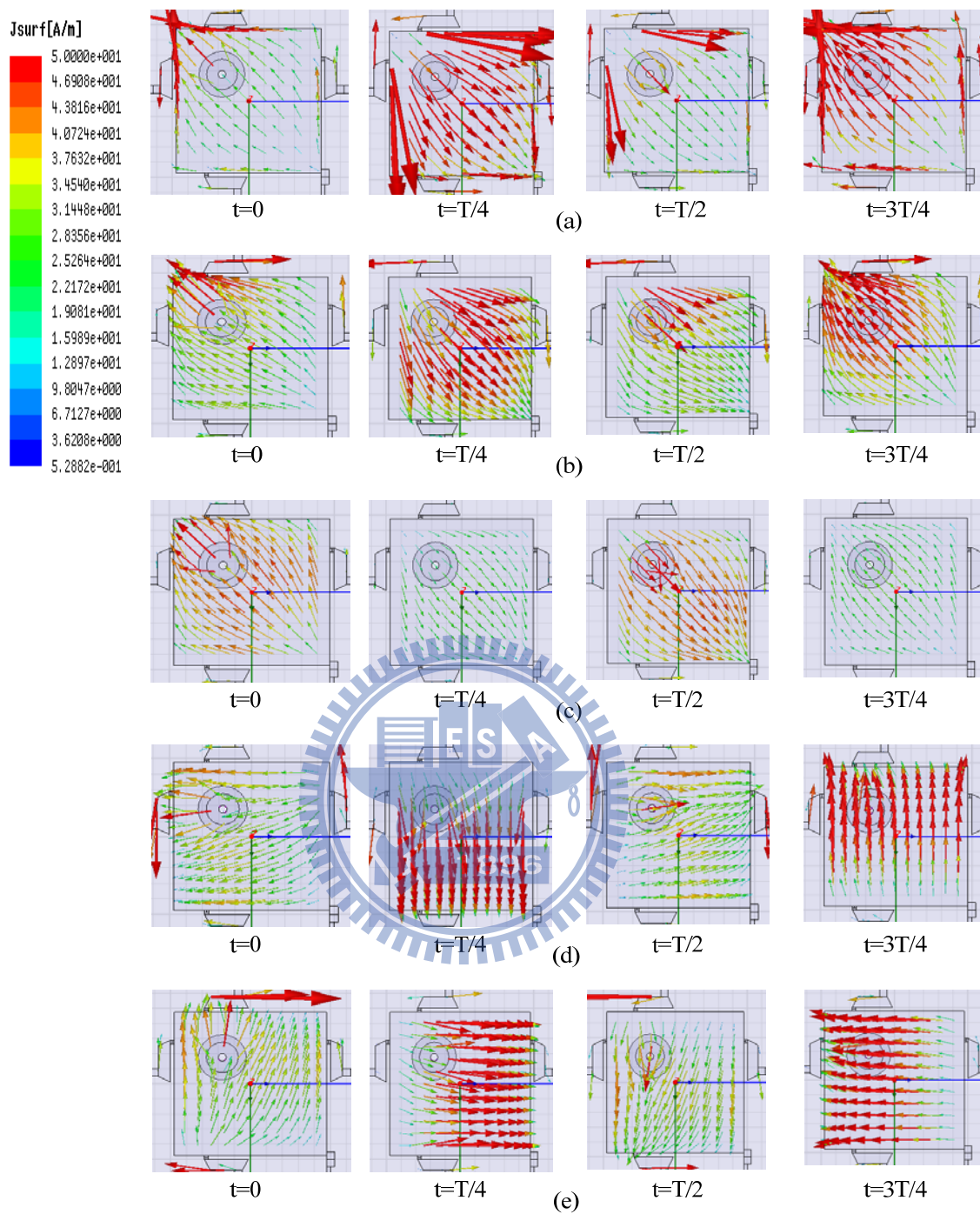


Fig. 3-10. Simulated surface current distribution of (a)  $FR_l$ , (b)  $FR_{mid}$ , (c)  $FR_h$ , (d)  $PR_{rhcp}$ , and (e)  $PR_{lhcp}$ .

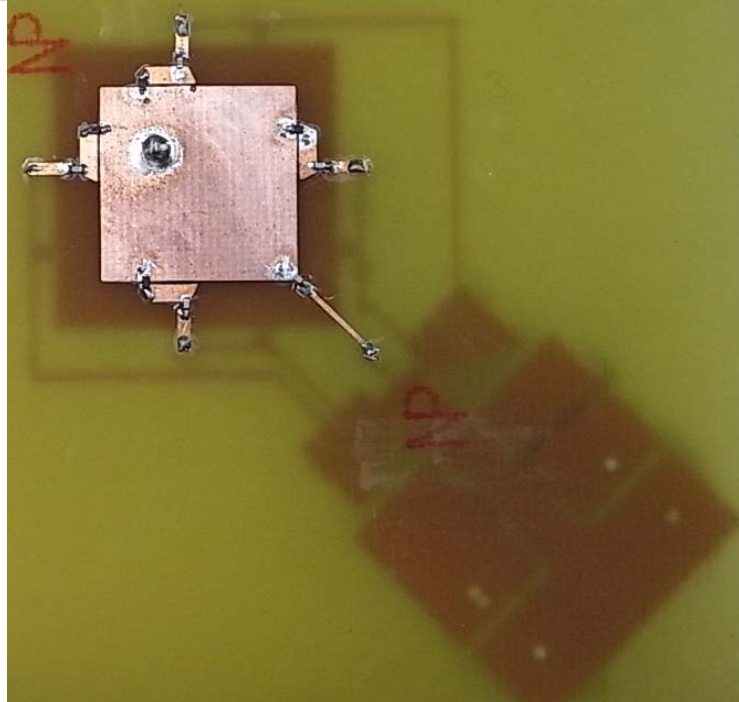
### 3.3 Parametric Study and Radiation Characteristics

#### 3.3.1 Parametric Study

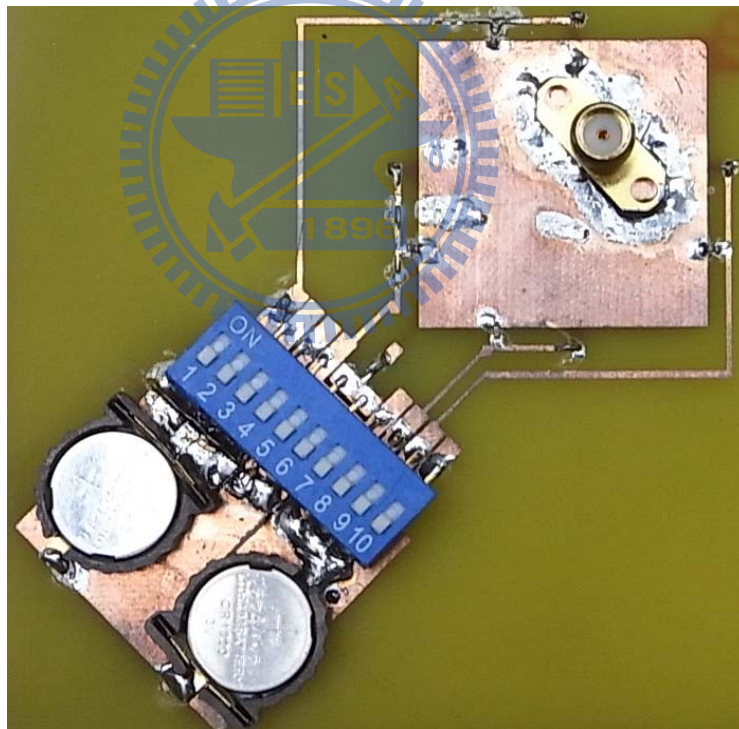
The parametric study is useful because it provides a comprehensive picture of the antenna characteristics. Because the each mechanism in FR or PR scheme are similar, FR<sub>l</sub>, PR<sub>lhcp</sub> are chosen in the following discuss for simplification. The shape of adjacent patches is firstly considered for the FR and PR schemes. For FR scheme, Fig. 3-7 show the effect of the shape of adjacent patches. As  $L_5$  and  $W_1$  increase, the longer current path causes the lower resonant frequency on each mode. Whereas, for PR scheme, the axial ratio is strong related current distribution in the adjacent patches as shown in Fig. 3-8. The position of diodes is another issue in our design. As shown in Fig. 3-9, the position of diode is slightly related with the resonant frequency and axial ratio. By the parameters study as show in Fig. 3-7, Fig. 3-8, and Fig. 3-9,  $W_1$ ,  $L_4$  and  $L_5$  are chosen for maintaining better operating bandwidth and polarization performance. Through trial-and-error to optimize the position and the shape of adjacent patches, the proposed antenna retains good impedance matching in each mode and fulfills the PR scheme with acceptable RHCP/LHCP bandwidth.

The simulated current distribution of each operation of FR and PR scheme firstly present in Fig. 3-10. According to Fig. 3-7(a) to (c), the proposed antenna operated in the FR scheme; they have similar current distributions in the FR scheme. As expected, a surface current remains linear movement along with the diagonal line in one periodicity. Whereas, as shown in Fig. 3-7 (d) and (e), it is clearly that the surface current rotates clockwise for PR<sub>lhcp</sub> or anticlockwise for PR<sub>rhcp</sub> in one periodicity.





(a)



(b)

Fig. 3-11. Photograph of (a) the front side and (b) the back side of fabricated antenna.

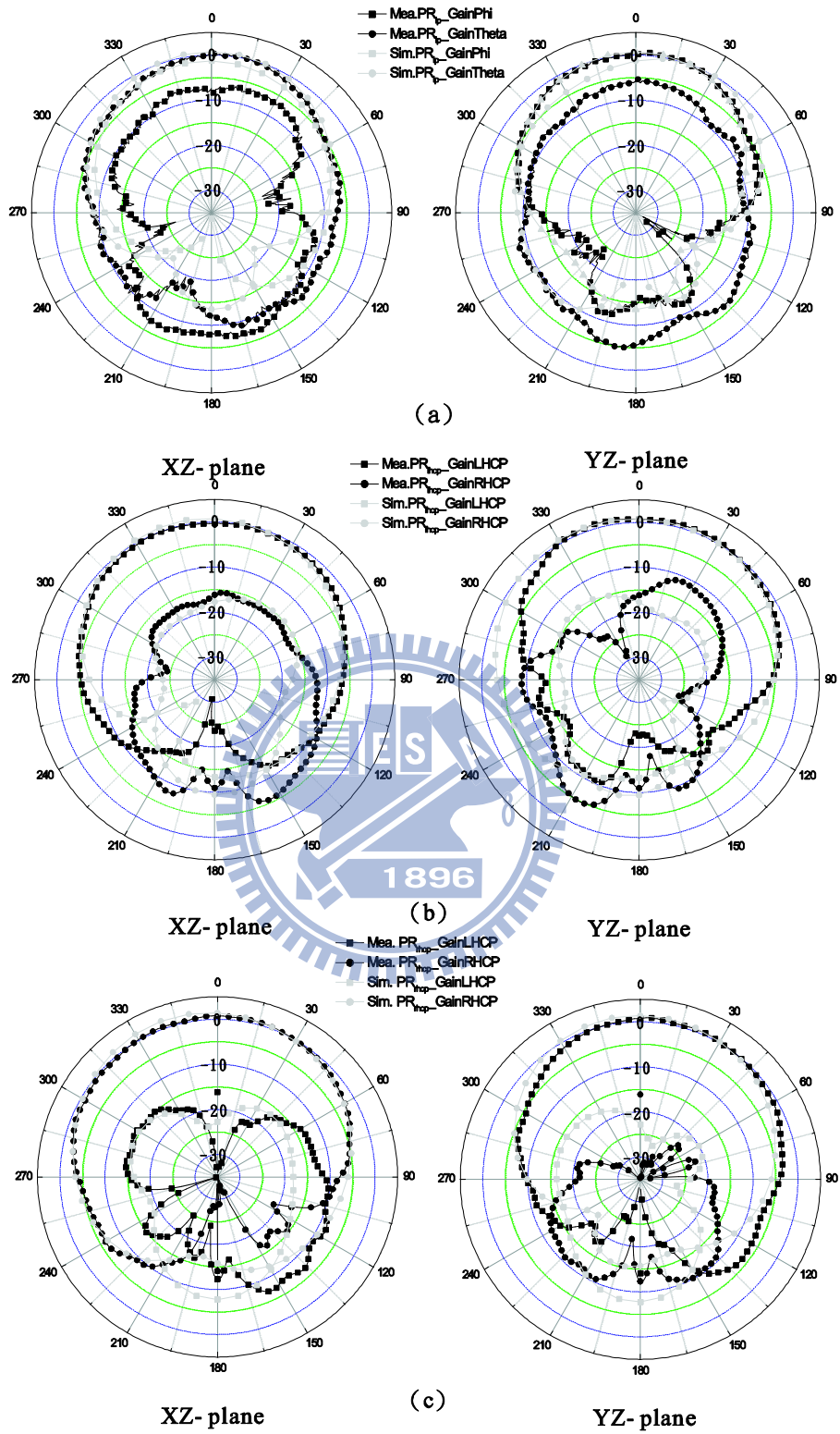


Fig. 3-12. Simulated and measured radiation patterns for (a)  $PR_{mid}$ , (b)  $PR_{lhcp}$ , and (c)  $PR_{rhcp}$  (unit : dBi)

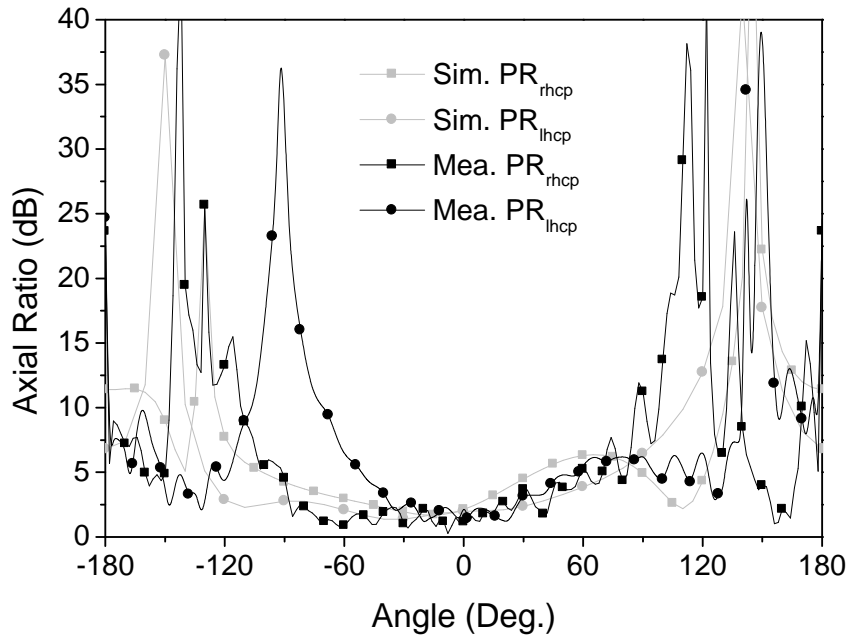


Fig. 3-13. The simulated and measured axial ratio at 3.35GHz for  $PR_{lhcp}$  and  $PR_{rhcp}$ .

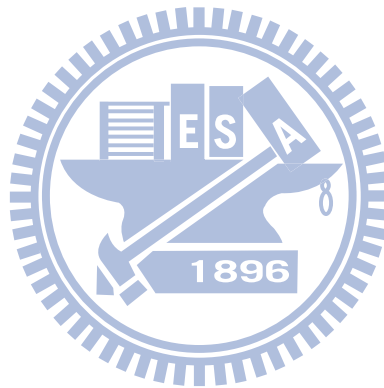
### 3.3.2 Radiation Characteristics

A photograph of the proposed antenna along with the bias network and SMA connector is shown in Fig. 3-11. The dc network and battery are attached at the bottom layer for the convenient measurement. The radiation patterns of each operation are shown in Fig. 3-12. As shown in the figures, the agreement between simulation and measurement is fairly well, and the slight discrepancy can be attributed to the fabrication tolerance, the interference from dc bias lines as well as the diodes model used in the simulation. Since the patterns of  $FR_h$ ,  $FR_l$  and  $FR_{mid}$  are quite similar, the Fig. 3-12 (a) only shows the patterns of  $FR_{mid}$  in xz-plane and yz-plane for simplification.

The measured backward radiation is a little bit higher than the simulated one, which is also likely a result of interference from the battery and finger switch that is not used in the simulation. Moreover, in Fig. 3-12 (b) and (c) show the radiation patterns of  $PR_{lpch}$  and  $PR_{rhcp}$  in the xz- and yz-plane. Good symmetry of radiation patterns along broadside direction is

shown.

Fig. 3-13 shows the measured and simulated AR at 3.35GHz for  $PR_{lpch}$  and  $PR_{rhcp}$  cases. The measured axial ratio at  $\theta=0^\circ$  in 3.35GHz is 1.2 for RHCP and 2.5 for LHCP. An accepted AR ( $\leq 3\text{dB}$ ) is obtained in broad angular range from  $-88^\circ$  to  $26^\circ$  for RHCP and  $-38^\circ$  to  $28^\circ$  for LHCP. The measured AR bandwidth is a little bit narrow, and both of measured  $S_{11}$  and AR of  $PR_{lhcp}$  slightly shifts higher than the simulated one, which may be attributed to fabrication tolerance.



## **Chapter 4**    *Conclusion*

---

A reconfigurable patch antenna for polarization and frequency diversities had been shown in Chapter 3. By proper switching PIN diodes on or off, the antenna can operate in  $FR_h$ ,  $FR_{mid}$  and  $FR_l$  for frequency diversity, and  $PR_{rhcp}$ ,  $PR_{lhcp}$  and  $PR_{lp}$  for polarization diversity. The design concept and operating mechanism have been analyzed and illustrated. In addition, the proposed antenna uses single probe feed without extra matching networks; therefore, it has compact size and simple structure, which is easier to fabricate. The simulation and measurement are agreement in this work.

SDR/CR devices need to changes its transmission or reception parameters including operating frequency, spectrum, and modulation to communicate efficiently between licensed and unlicensed users. By the reconfigurable frequency and polarization capabilities with the minimal number of diodes, the proposed antenna is suitable for cognitive radio and wireless communication applications.

## Appendix A. Introduction of Slot Antennas

---

The antenna shown in Fig. A-1 (a) consisting of two resonant quarter wavelength stubs connected to a two wire transmission line. the long wires are closely spaced ( $w \ll \lambda$ ) and carry currents of opposite phase so that their fields tend to cancel. The end wires carry currents in the same phase, but they are too short to radiate efficiently. In Fig. A-1(b), a half wavelength slot is cut in a flat metal sheet. Although the width of the slot is small ( $w \ll \lambda$ ), the currents are not confined to the edges of the slot but spread out over the sheet. Radiation occurs equally from both sides of the sheet. A slot antenna may be conveniently energized with a coaxial transmission line as in Fig. A-1 (c) or Fig. A-1 (d) for better impedance matching.

A microstrip-fed slot antenna, which consists of a microstrip line and a slot on the ground, uses microstrip-to-slot transition to excite the slot. Microstrip-to-slot transition has been widely used and analyzed by many investigators. A layout of this transition is shown in Fig. A-2.

A transmission line equivalent circuit of the transition (Fig. A-2.) proposed by *Chambers* is shown in Fig. A-3. The reactance  $X_{0s}$  represents the inductance of a shorted slot, and  $C_{0c}$  is the capacitance of an open microstrip.  $Z_{0s}$  and  $Z_{0m}$  are the slot and microstrip characteristic impedance respectively.  $\theta_s$  and  $\theta_m$  represent the electrical lengths (quarter-wave at the center frequency) of the extended portions of the slot and the microstrip, respectively,

measured from the reference planes as shown in Fig. A-3. The transformer turns ratio  $n$  represents the magnitude of the coupling between the microstrip and slot.

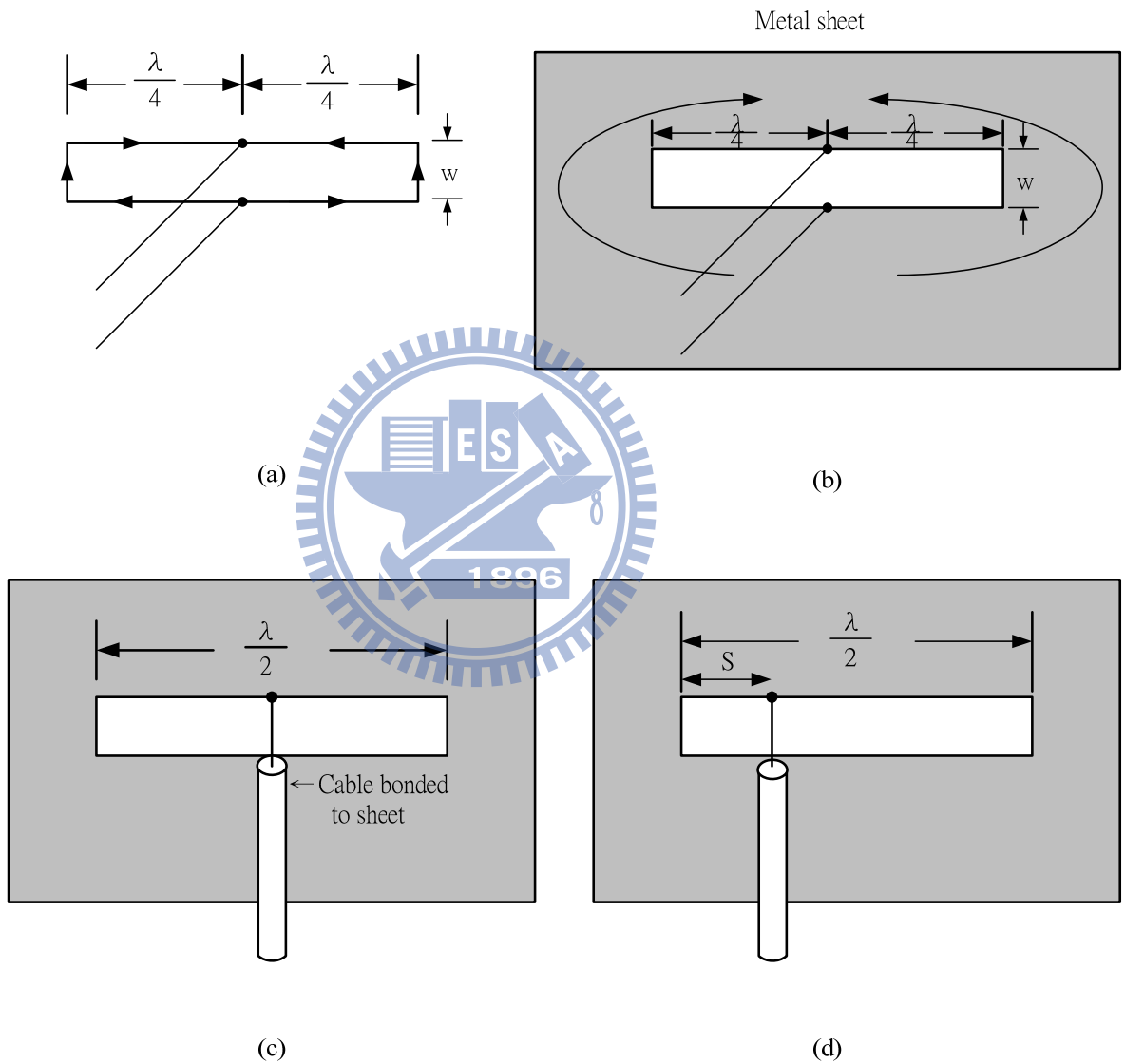


Fig. A-1. The stubs of (a) are a poor radiator, the slot of (b) is a good, efficient radiator. (c) and (d) are slot antennas fed by coaxial transmission lines.

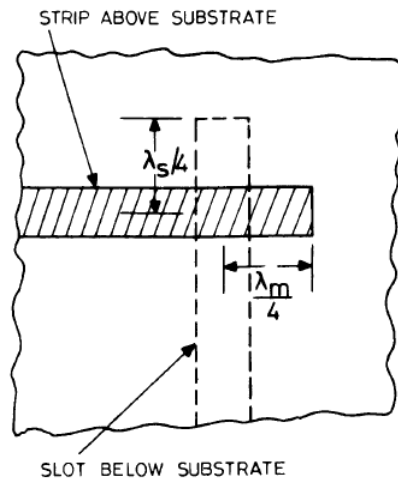


Fig. A-2. A layout of microstrip-to-slot transition

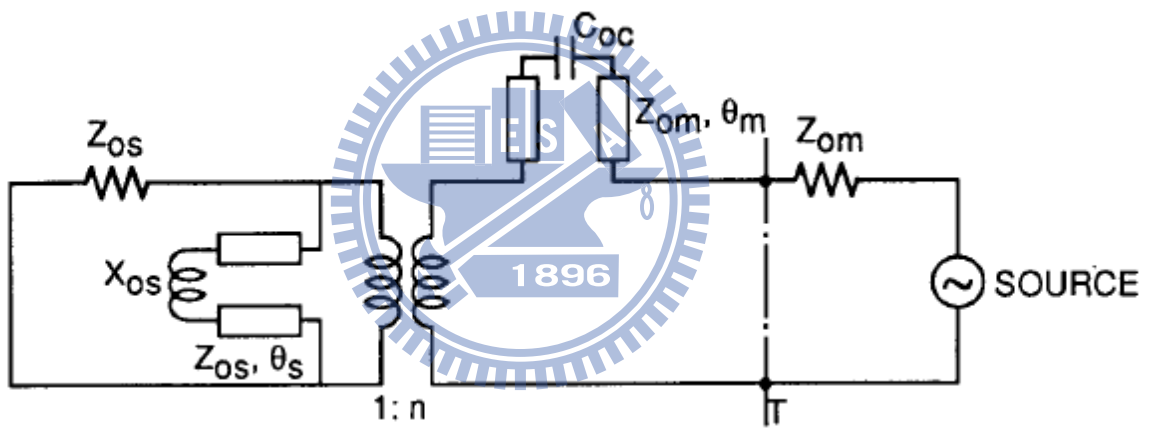


Fig. A-3. Transmission line equivalent circuit for the transition of Fig. A-2

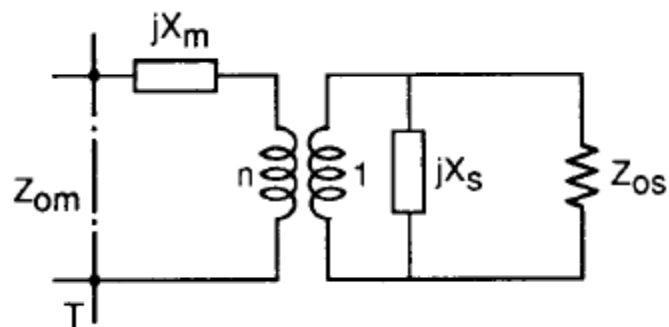


Fig. A-4. Reduced equivalent circuit of Fig. A-3.



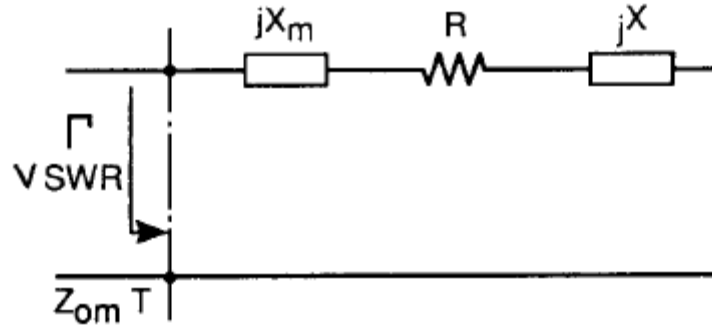


Fig. A-5. Transformed equivalent circuit of Fig. A-4

For further analysis the equivalent circuit in Fig. A-3 may be redrawn as in Fig. A-4. Here,

$$jX_s = Z_{0s} \frac{jX_{0s} + jZ_{0s} \tan \theta_s}{Z_{0s} - X_{0s} \tan \theta_s}$$

and

$$jX_m = Z_{0m} \frac{1/j\omega C_{0c} + jZ_{0m} \tan \theta_m}{Z_{0m} + \tan \theta_m / \omega C_{0c}}$$

After transformation to the microstrip side, the equivalent circuit of Fig. A-4 reduces to that shown in Fig. A-5. In this circuits,

$$R = n^2 \frac{Z_{0s} X_s^2}{Z_{0s}^2 + X_s^2}$$

and

$$X = n^2 \frac{Z_{0s}^2 X_s}{Z_{0s}^2 + X_s^2}$$

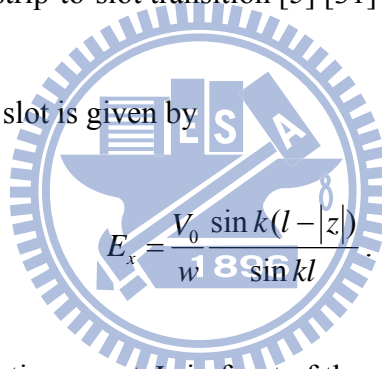
Finally, the reflection coefficient  $\Gamma$  is given by

$$\Gamma = \frac{R - Z_{0m} + j(X_m + X)}{R + Z_{0m} + j(X_m + X)}$$

From the above analysis, we can determine the characteristic impedance of the slot  $Z_{0s}$  to match the microstrip line impedance  $Z_{0m}$ .

Generally, the microstrip extends about one quarter of a wavelength beyond the slot or using a via to achieve microstrip-to-slot transition [5] [31] [33].

The electric field in the slot is given by



$$E_x = \frac{V_0 \sin k(l - |z|)}{w \sin kl}$$

This is identical to the magnetic current  $J_m$  in front of the ground plane.

$$J_m = \bar{E} \times \hat{n} = E_x \hat{x} \times \hat{y} = E_x \hat{z}$$

This is equivalent to the magnetic current  $J_m$  and its image in free space. Hence, the field is equal to the field generated by  $2J_m$ . Utilizing the following equations for radiation field  $E_\theta$

and  $E_\phi$  due to  $\bar{J}\left(\vec{r}'\right)$  and  $\bar{J}_m\left(\vec{r}'\right)$

$$E_\theta = -\frac{j\omega\mu_0}{4\pi R} e^{-jkR} \int \hat{\theta} \cdot \bar{J}\left(\vec{r}'\right) e^{jk\hat{r} \cdot \vec{r}'} dV' - \frac{jk}{4\pi R} e^{-jkR} \int \hat{\phi} \cdot \bar{J}_m\left(\vec{r}'\right) e^{jk\hat{r} \cdot \vec{r}'} dV'$$

$$E_\phi = -\frac{j\omega\mu_0}{4\pi R} e^{-jkR} \int \hat{\phi} \cdot \bar{J}\left(\vec{r}'\right) e^{jk\hat{r} \cdot \vec{r}'} dV' + \frac{jk}{4\pi R} e^{-jkR} \int \hat{\theta} \cdot \bar{J}_m\left(\vec{r}'\right) e^{jk\hat{r} \cdot \vec{r}'} dV'$$

We have

$$E_{\theta} = 0$$

$$E_{\phi} = -j \frac{e^{-jkR}}{\pi R} V_0 \frac{\cos(kl \cos \theta) - \cos kl}{\sin kl \sin \theta}$$

The magnetic field  $\vec{H}$  in the far field is simply related to  $\vec{E}$  :

$$\vec{H} = \frac{1}{\eta} \hat{r} \times \vec{E}, \quad \eta = \sqrt{\frac{\mu_0}{\epsilon_0}}$$

Therefore,

$$H_{\theta} = -\frac{E_{\phi}}{\eta} = j \frac{e^{-jkR}}{\eta \pi R} V_0 \frac{\cos(kl \cos \theta) - \cos kl}{\sin kl \sin \theta}$$

$$H_{\phi} = \frac{E_{\theta}}{\eta} = 0$$

Since 2004, the reduced-size quarter wavelength slot antennas have been proposed in [36]-[39]. A common schematic diagram is shown in Fig. A-6 [36][37]. The length of the slot,  $L_s$ , is about a quarter guided -wavelength.

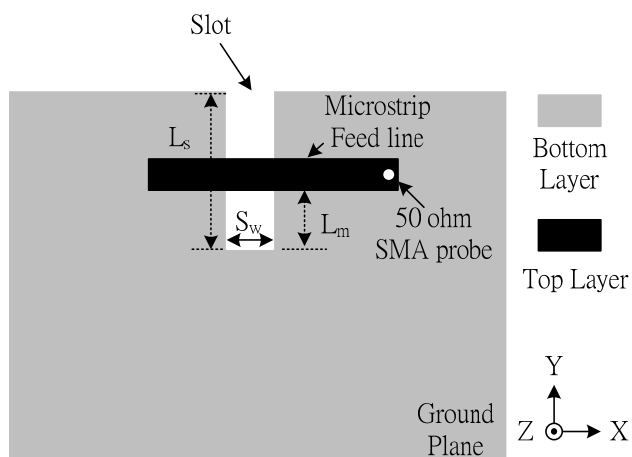


Fig. A-6. Geometry of a microstrip-fed quarter-wavelength slot antenna.



## **Appendix B. *Frequency Reconfigurable Slot Antenna***

### ***Using PIN Diodes***

---

#### **B.1 Introduction**

As mentioned in Chapter 1, with the rapid development of wireless communication systems, the reconfigurable antenna technologies have received significant attentions in the world. To cooperate well with the wireless devices, the reconfigurable antenna features higher integration density, multiple functionality, reconfigurable capability and low cost properties. The reconfigurable antenna commonly adapts their properties to achieve selectivity in frequency, bandwidth and radiation polarization. To achieve operation in several frequency bands or enhance the available bandwidth, the frequency reconfigurable antenna changes operating frequency for several services while maintaining radiation characteristics [30]-[32].

In this chapter, we propose a frequency reconfigurable slot antenna. The proposed structure is based on an open-end straight slot line and the PIN diodes to achieve frequency reconfigurable capability. The PIN diodes along with DC bias network are located at specific positions to create short circuit or open circuit across the slot. By carefully controlling these diodes, the antenna operates as the conventional  $\lambda/4$  slot antenna. The proposed antenna structure and design concept are presented in B.2. B.3 provides the measured and simulated results of the proposed antenna such as return loss and radiation patterns. Finally, 錯誤! 找

不到參照來源。 gives a brief summary.

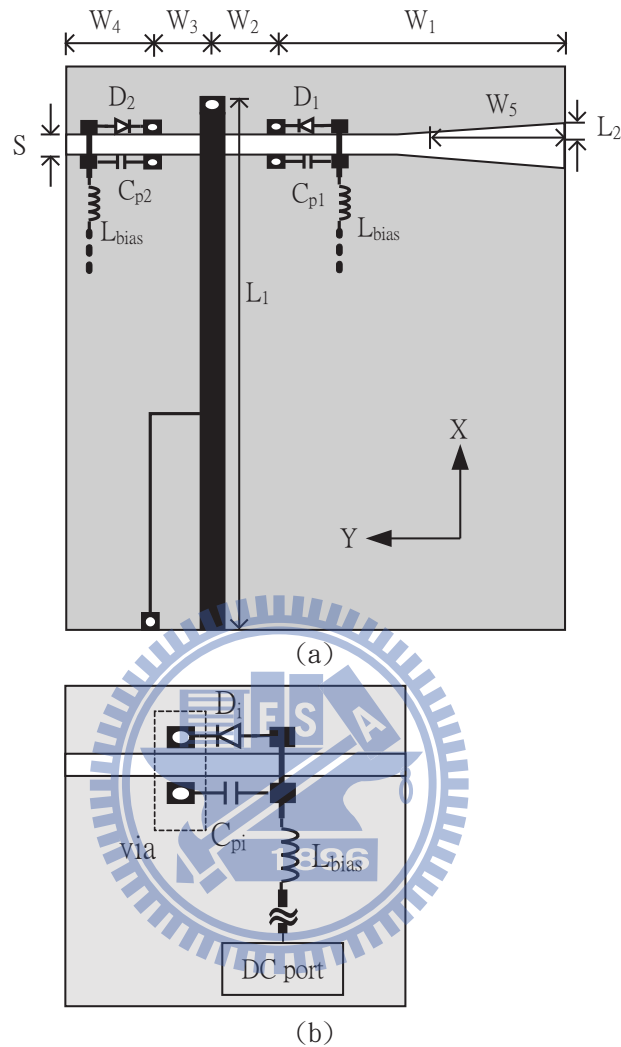


Fig. B-1. (a) Configuration of proposed antenna. (b) PIN diodes arrangement and the associated dc bias network.

## B.2 Antenna Configuration and Design Concept

Fig. B-1 depicts the proposed antenna configuration and the layout of bias network. The antenna is excited using a short-circuited microstrip line fed by an SMA connector. The antenna consists of a straight slot line on the bottom layer, two PIN diodes, two lumped capacitors, and bias network. Additionally, a quarter-wavelength short-circuit stub is added to the microstrip line to avoid that the metal sheet which is created by the slot is floating. The

Fig. B-1. (b) shows the layout of the diodes and the DC bias network. The slot line and the dc network are isolated by  $L_{\text{bias}}$ . The  $C_{p1}$  and  $C_{p2}$  are used to support the necessary DC isolation between the both metal sheets on the group plane.

In the design concept, the frequency reconfigurable capacity of the proposed antenna mostly depends on length from open end slot to the forward state diode. According to Fig. B-1 (a), the lengths of  $W_1+W_2+W_3$ ,  $W_2+W_3+W_4$  are approximately quarter wave length of 2.45GHz and 2.9GHz.  $D_1$ ,  $D_2$ ,  $C_{p1}$  and  $C_{p2}$  located at specific positions are used to switch the operating frequencies. When the antenna is operated at 2.45GHz or 2.9GHz, the  $C_{p1}$  and  $C_{p2}$  behave the zero resistance lump circuit. It should be noted that the position of the diodes and the capacitors are also used to well match the impedance in our design.

The proposed antenna operates at two modes, i.e., the right side radiated mode (RR mode) and the left side radiated mode (LR mode). The operating frequency of the proposed antenna at the RR mode is 2.45 GHz and at the LR mode is 2.9 GHz. When the proposed antenna operates at the RR mode,  $D_1$  is at reversed state and  $D_2$  at forward state and then the wave radiates to -y axis. In reversely, as  $D_1$  is at forward state and  $D_2$  is at reversed state, the wave radiates to y axis at the LR mode. According to our design experiment, at each mode, the forward state diode can be used for good impedance matching and reverse state diode is not significant influence.

### **B.3 Simulated and Measured Results**

The simulation is performed using Ansoft HFSS while the measurement is taken by an Agilent E8362B performance network analyzer. The patterns of the proposed antenna are measured in a 7.0 x 3.6 x 3.0 m<sup>3</sup> anechoic chamber with the NSI far-field measurement software. The proposed antenna is fabricated on a FR4 substrate with a dielectric constant of 4.4 and thickness of 0.8mm. The loss tangent of substrate is 0.02. The optimized parameters

are as follows:  $W_1=13.75$ ,  $W_2=W_3=3.95$ ,  $W_4=4.75$ ,  $W_5=9.7$ ,  $W_6=1.4$ ,  $S=1$ ,  $L_1=37$ ,  $L_2=1$ , unit mm. The overall dimension of the proposed design is  $26.4 \times 40$  mm<sup>2</sup>. In the following design Infineon BAR64-02V PIN diodes are used, with a forward resistance of 2.1ohm, a reverse parallel resistance of 3000 ohm, a diode capacitance of 0.17pF, and a lead inductance of 0.6nH. The value of  $C_{p1}$  and  $C_{p2}$  are 2.2pF while the  $L_{bias}$  is 100nH.

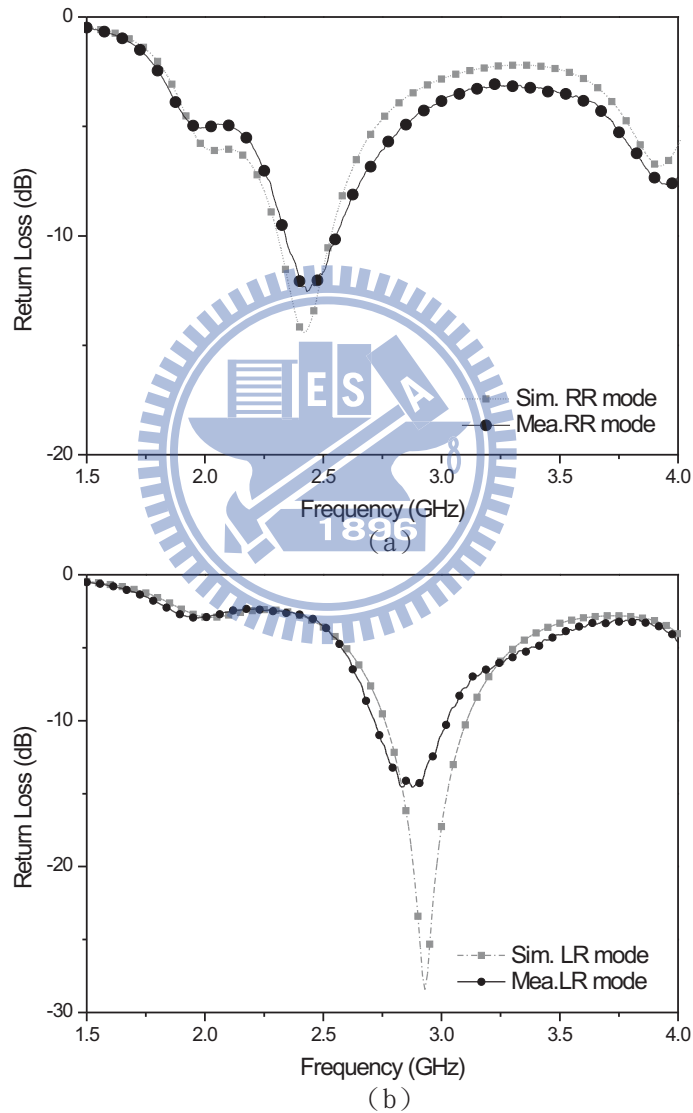


Fig. B-2. Return loss of proposed antenna. (a) LR mode. (b) RR mode.

Fig. B-2 exhibits the simulated and measured return loss at the RR mode and the LR mode. As shown in the figures, the agreement between the simulation and measurement is fairly well, and the slight discrepancy can be attributed to the fabrication tolerance, the



interference from the dc bias lines and connecting cable, as well as from the diodes model used in the simulation. The proposed antenna can operate at different frequencies by controlling the positions of the diodes.

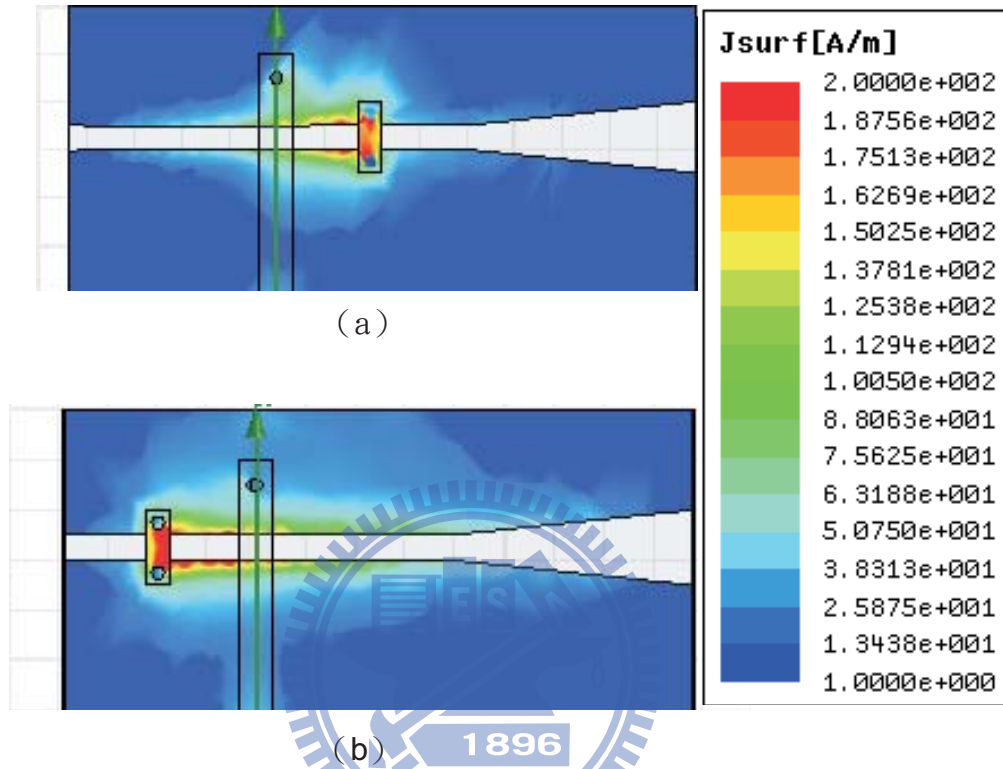


Fig. B-3. Simulated current distribution, (a) LR mode. (b) RR mode.

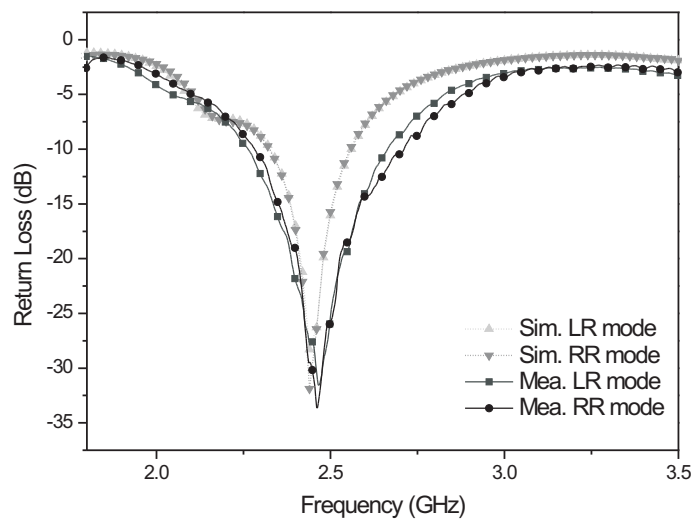


Fig. B-4. Return loss of proposed antenna at  $W_1=W_4=13.75\text{mm}$

The simulated current distribution at RR mode and LR mode are shown in Fig. B-3. It is obvious that they both closed follow a quarter sinusoidal pattern with the maximum current concentrated in the forward state diode and the minimum current in the open-end slot. It should be mentioned that the two modes share very similar properties and the antenna structure can be applied in other operating frequencies.

According our design concept, the proposed antenna is not only treated as the frequency reconfigurable antenna, but also is treated as the pattern reconfigurable antenna when both length of slots at right side and left side are equal. The Fig. B-4 shows the measured and simulated return loss of proposed antenna when left side structure is as same as right side structure of the antenna. In this case, at RR mode and LR mode, the operating frequencies are both 2.45 GHz. and the wave radiates to opposite directions.

Fig. B-5 exhibits the simulated and measured radiation patterns of the RR mode and the LR mode in xy-,and yz-plane. The measured patterns agree with the simulation results. The measured gain in the yz-plane at RR mode (2.45 GHz) and the LR mode (2.9 GHz) is -0.6 dBi and 0.093 dBi, respectively. The measured gains are slight lower than the simulated ones, mainly resulting from the PIN diodes and DC bias network. the cross-polarization levels are generally much lower than the co-polarization ones. The proposed antenna also show good front-to-back ratio at yz- and xy-plane.

## **B.4 Conclusion**

A frequency-reconfigurable slot antenna has been proposed in Appendix B. By carefully controlling these diodes, the antenna behaves conventional  $\lambda/4$  slot antenna. According to the length form the open-end slot line to the microstrip line and the position of the forward state diode, the proposed antenna can operate at assigned frequencies with opposite radiated direction at the RR mode and the LR mode. The measured results agree with the simulated

ones. The maximum radiated gain is around 0.93 dBi for 2.45GHz and 0.95 dBi for 2.9 GHz. The proposed antenna may apply in various forms of the wireless communication.



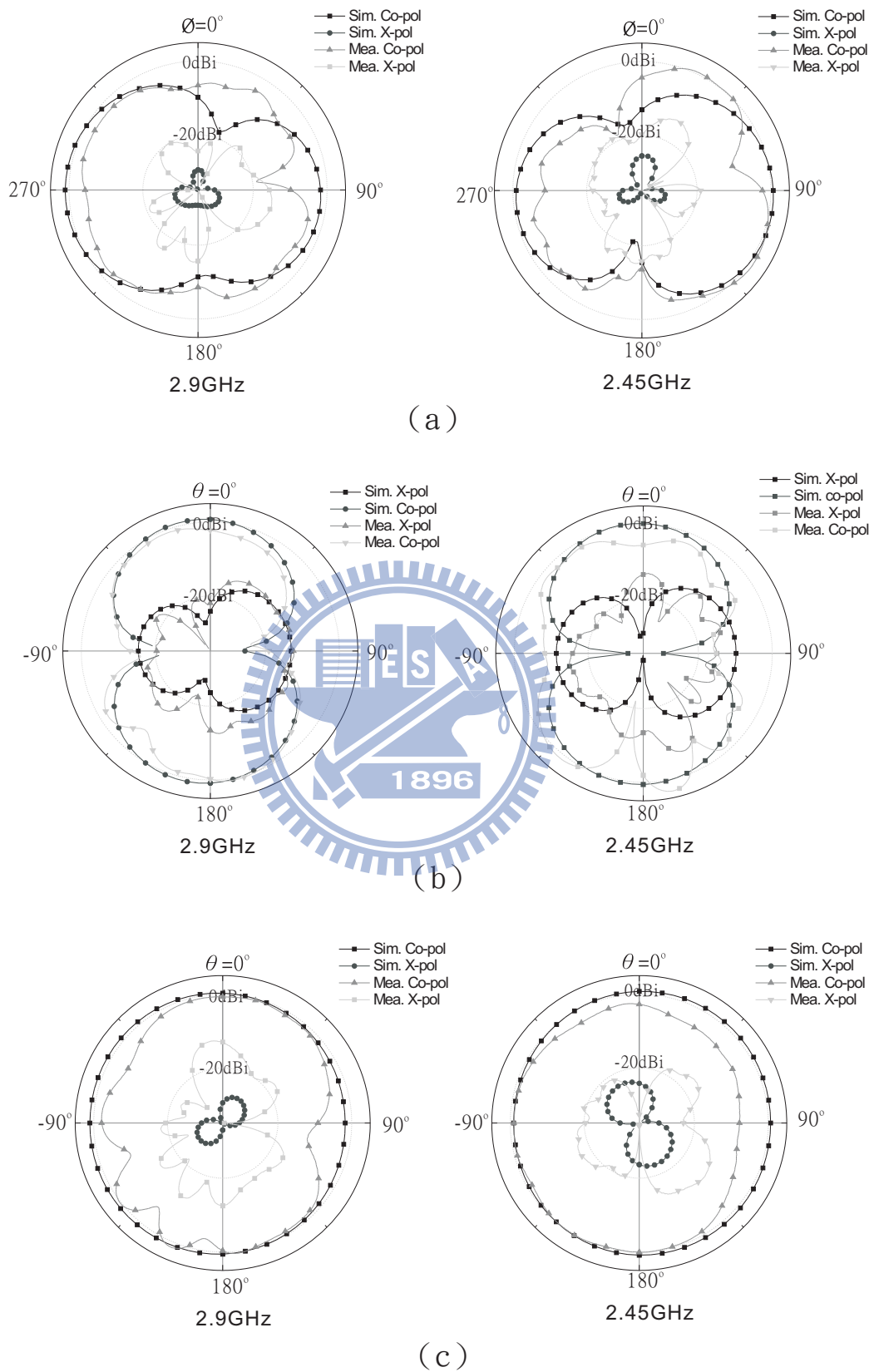


Fig. B-5. Simulated and measured radiation patterns. (a) xy-plane. (b) xz-plane. (c) yz-plane.

---

---

## References

---

- [1] P.H. Rao, "Antenna configurations for software defined radio and cognitive radio communication architecture," *Wireless Communication and Sensor Computing, 2010. ICWCSC 2010. International Conference on*, pp.1-4, 2-4 Jan. 2010
- [2] S. Yang, C. Zhang, H. K. Pan, A. E. Fathy, and V. K. Nair, "Frequency-reconfigurable antennas for multiradio wireless platforms," *IEEE Microwave Magazine*, vol.10, no.1, pp.66-83, February 2009
- [3] D. Peroulis, K. Sarabandi, and L. P. B. Katehi, "Design of reconfigurable slot antennas," *IEEE Trans. Antennas Propag.*, vol. 53, pp. 645–654, Feb. 2005.
- [4] F. Yang and Y. Rahmat-Samii, "Patch antenna with switchable slots (PASS): reconfigurable design for wireless communications, " in *Proc. IEEE Antennas and Propag. Society Int. Symp.*, vol.1, pp. 462- 465, 2002
- [5] K. H. Chen, S. J. Wu, C. H. Kang, C. K. Chan, and J. H. Tarng, "A frequency reconfigurable slot antenna using PIN diodes," in *Proc. Asia-Pacific Microw. Conf.*, pp.1930-1933, 7-10 Dec. 2009
- [6] M. I. Lai, T. Y. Wu, J. C. Hsieh, C. H. Wang, and S. K. Jeng, "Compact Switched-Beam Antenna Employing a Four-Element Slot Antenna Array for Digital Home Applications," *IEEE Trans. Antennas Propag.*, vol.56, no.9, pp.2929-2936, Sept. 2008
- [7] S. H. Chen, J. S. Row, and K. L. Wong, "Reconfigurable Square-Ring Patch Antenna With Pattern Diversity," *IEEE Trans. Antennas Propag.*, vol.55, no.2, pp.472-475, Feb. 2007

- [8] S. Nikolaou, R. Bairavasubramanian, C. L. Jr, I. Carrasquillo, D. C. Thompson, G. E. Ponchak, J. Papapolymerou, and M. M. Tentzeris, "Pattern and frequency reconfigurable annular slot antenna using PIN diodes," *IEEE Trans. Antennas Propag.*, vol.54, no.2, pp. 439- 448, Feb. 2006
- [9] S. J. Wu and T. G. Ma, "A Wideband Slotted Bow-Tie Antenna With Reconfigurable CPW-to-Slotline Transition for Pattern Diversity," *IEEE Trans. Antennas Propag.*, vol.56, no.2, pp.327-334, Feb. 2008
- [10] A. Grau, J. Romeu, M. J. Lee, S. Blanch, L. Jofre, and F. D. Flaviis, "A Dual-Linearly-Polarized MEMS-Reconfigurable Antenna for Narrowband MIMO Communication Systems," *IEEE Trans. Antennas Propag.*, vol.58, no.1, pp.4-17, Jan. 2010
- [11] Y. J. Sung, "Reconfigurable Patch Antenna for Polarization Diversity," *IEEE Trans. Antennas Propag.*, vol.56, no.9, pp.3053-3054, Sept. 2008
- [12] E. Nishiyama and M. Aikawa, "Circular polarization controllable microstrip antenna," in *Proc. IEEE Antennas and Propag. Society Int. Symp.*, pp.5195-5198, 9-15 June 2007
- [13] Y. Ushijima, E. Nishiyama, and M. Aikawa, "Wide band switchable circularly polarized microstrip antenna using double-balanced multiplier," in *Proc. IEEE Antennas and Propag. Society Int. Symp.*, pp.1-4, 5-11 July 2008
- [14] J. Ouyang, F. Yang, and S. Yang, "A novel reconfigurable circular polarization patch antenna," *Microw. Opt. Technol. Lett.*, vol. 50, pp. 1921-1923, 2008.
- [15] F. Ferrero, C. Luxey, R. Staraj, G. Jacquemod, M. Yedlin, and V. Fusco, "A Novel Quad-Polarization Agile Patch Antenna," *IEEE Trans. Antennas Propag.*, vol.57, no.5, pp.1563-1567, May 2009
- [16] Y. F. Wu, C. H. Wu, D. Y. Lai, and F. C. Chen, "A Reconfigurable Quadri-Polarization Diversity Aperture-Coupled Patch Antenna," *IEEE Trans. Antennas Propag.*, vol.55, no.3, pp.1009-1012, March 2007
- [17] Y. J. Sung, T. U. Jang, and Y. S. Kim, "A reconfigurable microstrip antenna for switchable polarization," *IEEE Microw. Wireless Compon. Lett.*, vol. 14, pp. 534-536,

- Nov. 2004.
- [18] M. S. Parihar, A. Basu, and S. K. Koul, "Polarization reconfigurable microstrip antenna," in *Proc. Asia-Pacific Microw. Conf.*, pp.1918-1921, 7-10 Dec. 2009
- [19] F. Yang and Y. Rahmat-Samii, "Patch antennas with switchable slots (PASS) in wireless communications: concepts, designs, and applications," *IEEE Antennas Propag. Mag.*, vol.47, no.2, pp. 13- 29, April 2005
- [20] R. H. Chen and J. S. Row, "Single-Fed Microstrip Patch Antenna With Switchable Polarization," *IEEE Trans. Antennas Propag.*, vol.56, no.4, pp.922-926, April 2008
- [21] N. Jin, F. Yang, and Y. Rahmat-Samii, "A novel patch antenna with switchable slot (PASS): dual-frequency operation with reversed circular polarizations," *IEEE Trans. Antennas Propag.*, vol.54, no.3, pp.1031-1034, March 2006
- [22] K. R. Carver and J. W. Mink, "Microstrip Antenna Technology," *IEEE Trans. Antennas & Propagation*, Vol. AP-29, pp. 2-24, Jan. 1981.
- [23] R. E. Munson, "Conformal Microstrip Antennas and Microstrip Phase Arrays," *IEEE Trans. Antennas & Propagation*, Vol. AP-22, pp. 74-78, Jan.1974
- [24] D. H. Schaubert, "Microstrip Antennas," *Electromagnetics*, Vol. 12, pp. 381-401, July-December 1992.
- [25] K. Chung, Y. Nam, T. Yun, and J. Choi, "Reconfigurable microstrip patch antenna with switchable polarization," *ETRI Journal*, vol. 28, 379-382, Jun. 2006.
- [26] B. Kim, B. Pan, S. Nikolaou, Y. S. Kim, J. Papapolymerou, and M. M. Tentzeris, "A Novel Single-Feed Circular Microstrip Antenna With Reconfigurable Polarization Capability," *IEEE Trans. Antennas Propag.*, vol.56, no.3, pp.630-638, March 2008
- [27] W. F. Richards, Y. T. Lo, and D. D. Harrison, "An improved theory for microstrip antennas and applications," in *Proc. IEEE Antennas and Propag. Society Int. Symp.*, vol.17, no., pp. 113- 116, Jun 1979
- [28] W. F. Richards, Y. T. Lo, and P. Simon, "Design and theory of circularly polarized

- microstrip antennas," in *Proc. IEEE Antennas and Propag. Society Int. Symp.*, vol.17, pp. 117- 120, Jun 1979
- [29] B. Y. Toh, R. Cahill, and V. F. Fusco, "Understanding and measuring circular polarization," *IEEE Trans. Education*, vol.46, no.3, pp. 313- 318, Aug. 2003
- [30] N. Behdad, K. Sarabandi, "A varactor-tuned dual-band slot antenna," *IEEE Trans. Antennas Propag.*, vol.54, no.2, pp. 401-408, Feb. 2006.
- [31] D. Peroulis, K. Sarabandi, and L.P.B.Katehi, "Design of reconfigurable slot antennas," *IEEE Trans. Antennas Propag.*, vol.53, no.2, pp.645-654, Feb. 2005.
- [32] T. Debgovic, A. Karabelj, and J. Bartolic, "Dual band reconfigurable slot antenna with high frequency ratio," *Microwaves, Radar and Remote Sensing Symposium*, 2008. MRRS 2008 , vol., no., pp.22-25, 22-24 Sept. 2008.
- [33] K.C. Gupta, R. Garg, I.Bahl, P. Bhartia, *Microstrip Lines and Slotlines*, 2nd ed., Artech House, Boston, MA, 1996.
- [34] W. L. Stutzman and G. A. Thiele, *Antenna Theory and Design*, 2nd ed. New York: Wiley, 1998.
- [35] C. A. Balanis, *Antenna Theory Analysis and Design*, 3rd ed. New York: Wiley, 2005.
- [36] S. K. Sharma, L.Shafai, and N. Jacob, "Investigation of wide-bnd microstrip slot antenna," *IEEE Trans. Antenna and Propag.*, vol. 52, no. 3, pp. 965-872, Mar. 2004.
- [37] S.I. Latif, L. SHafai, and S. K. Sharma, "Bandwidth enhancement and size reduction of microstrip slot antennas," *IEEE Trans. Antennas and Propag.*, vol. 53, no. 3, pp. 994-1003, Mar. 2005.
- [38] A. P. Zhao and J. Rahola, "Quarter-wavelength widebend slot antenna for 3-5GHz moile applications," *IEEE Antennas and Wireless Propag. Lett.*, vol. 4, pp.421-424, 2005.
- [39] W. S. Chen and K.Y. Ku, "Broadband design of a small non-symmetric ground  $\lambda/4$  open slot antenna," *Microwave Journal*, vol. 50, no.1, pp. 110-121, Jan. 2007.